FINITE ELEMENT ANALYSIS OF HELICOPTER MAIN ROTOR HUB PLATES TO EVALUATE THE POSSIBILITY OF INCREASING THE TIME TO RETIREMENT

by

DOUGLAS WITTIG

Presented to the Faculty of the Graduate School of

The University of Texas at Arlington in Partial Fulfillment

of the Requirements

for the Degree of

MASTER OF SCIENCE IN MECHANICAL ENGINEERING

THE UNIVERSITY OF TEXAS AT ARLINGTON

December 2008

ACKNOWLEDGEMENTS

My first acknowledgement goes to my enduring and supportive wife Sheridan. Her encouragement, unconditional love, and toleration during a long and tedious masters program needs to be recognized.

I would also like to dedicate this to my dad who passed away in May 2008. He was very consistent in encouraging all of his children to obtain the highest education that was within their capabilities. He was there when I completed my undergraduate degree. I think he would have enjoyed this accomplishment as well.

I would like to express my gratitude to my co-workers who allowed me to work on this project and who also obtained funding. I would like to thank my research advisor, Dr. Kent Lawrence for his assistance and guidance.

November 17, 2008

ABSTRACT

FINITE ELEMENT ANALYSIS OF HELICOPTER MAIN ROTOR HUB PLATES TO EVALUATE THE POSSIBILITY OF INCREASING THE TIME TO RETIREMENT

Douglas Wittig, M.S.

The University of Texas at Arlington, 2008

Supervising Professor: Dr. Kent Lawrence

Rotorcraft main rotor systems have multiple components that are subject to very high loads and moments. These loads and moments dictate the life expectancy of the parts based upon the components material of composition. This project will focus on the upper and lower hub plates on the main rotor system of a typical four bladed commercial helicopter. The upper and lower plates are machined from 7075-T73 aluminum forgings. The upper and lower plates were laboratory fatigue tested during product development as supporting parts in the test of the main rotor assembly. With recent advances in finite element analysis, there are situations were a computer generated three dimensional model analysis would be more economical and time beneficial to determine if the life expectancy of a part can be increased above the

published safe life component retirement time. The applied loads are measured flight loads under maximum peak conditions and also ground-air-ground cycle loads. The stress values obtained from the loads are plotted on a Soderberg diagram and evaluated to determine if the retirement time of the part can be increased above the current value based on the steady and oscillatory stresses encountered.

TABLE OF CONTENTS

LIST OF ILLUSTRATIONS

LIST OF TABLES

CHAPTER 1

INTRODUCTION

1.1 Thesis Introduction

Finite Element (FE) analysis has become a very valuable tool to today's engineers. With recent advances in computer technology, the finite element software programs available today are more powerful and accurate than they were just eight to ten years ago. The use of FE analysis has become a common and highly accepted form in determining stresses and fatigue life of aircraft parts. With the ability to generate three dimensional part models with computer aided drawings, parts can easily be transferred to a FE software program to perform necessary analysis.

The most effective way to perform an FE analysis is to simulate all loads and boundary conditions that will exist in actual operating environments. From these conditions, the resulting stresses and deformations can be documented and the results compared to the mechanical material properties of the parts being analyzed. Performing FE analysis requires the engineer to be very familiar with the options available in the FE software. Being able to determine what kind of element type to use, mesh density, element sizing, and polynomial order are just a few items that the engineer must determine in order for the analysis to produce useful and effective results. In general a FE analysis is a trial and error method, particularly if a complex model is involved. In most cases it may be necessary to run several conditions in order to determine where the

area of high stress concentration or deformation occurs in the part. Once this is determined, the engineer can perform a mesh refinement on the areas of concern to get a more accurate analysis.

1.2 Project Overview

Rotorcraft main rotor systems have multiple components that are subject to very high loads and moments. These loads and moments dictate the life expectancy of the parts based upon the components material of composition. This project will primarily focus on the upper and lower hub plates on the main rotor system. The upper and lower plates are machined from 7075-T73 aluminum forgings. The upper and lower plates were laboratory fatigue tested as supporting parts in the test of the main rotor assembly. With recent advances in finite element analysis there are situations were a computer generated three dimensional model analysis would be more economical and time beneficial to determine if the life expectancy of a part can be increased. The objective of this project is to analyze a computer generated finite element analysis in lieu of a laboratory fatigue test to see if the fatigue life can be increased.

A three dimensional CATIA model of the upper and lower plates was used in performing the finite element analysis. The finite element analysis software used in this project is ANSYS. The loads applied to the parts are measured flight loads under maximum peak conditions and also ground-air-ground cycle loads. Once the loads are applied to the parts, the results from the finite element analysis are evaluated based on material mechanical allowable stress values. These values are then plotted on a Soderberg diagram and evaluated to determine if the fatigue life of the parts can be

increased based on the steady and oscillatory stresses encountered. The results obtained from the laboratory fatigue test can be used as a comparison to verify and substantiate the accuracy of the results obtained from the finite element analysis.

1.3 Objective and Outline of this Thesis

The objective of this thesis is to determine by FE analysis if the life expectancy of the upper and lower hub plates of the main rotor system can be increased above the current value. The maximum and minimum peak flight loads were applied to the FE model. The steady and oscillatory stresses were calculated and plotted on a Soderberg diagram to determine the life expectancy of the parts. This thesis is divided into five chapters. Chapter 1 introduces the topic material. Chapter 2 gives a background into similar research approaches using finite element analysis. Chapter 3 gives a detailed description of the methodology used to substantiate the results for the upper and lower hub plates. Chapter 4 discusses the results obtained from the finite element analysis. The areas with the highest stress concentration are closely evaluated and a summary showing all pertinent data is presented. Finally, a conclusion and recommendation is presented in Chapter 5.

CHAPTER 2

BACKGRGOUND

2.1 Literature Review

The use of finite element analysis has increased dramatically over the past ten years. With the advancements in computer processing speeds and software application algorithms, finite element analysis is becoming more common in the tools available to the engineer. The accuracy and adaptability of finite element analysis makes it utilizable over many different disciplines. The functionality of finite element analysis in pre-design, design modification, and design optimization makes it a powerful platform in engineering work. Finite element analysis allows engineers to perform analytical calculations and obtain results in a remarkably short period of time compared to a full scale testing. Every day civil, mechanical, aerospace, electrical, and automotive engineers use finite element analysis to perform tasks that were considered unimaginable decades ago.

Not only is this tool valuable to engineers, it is also utilized by other professions as well. Finite element analysis is used in the medical, dental, biomechanical, and orthopedic professions as well to name a few. Because of the increasing popularity, finite element analysis has had a very positive impact on the quality of products and on their longevity of use. One instance of increasing product quality was shown by Pegoretti [1]. He used finite element analysis to compare endodontic posts to compare a

cast metal post to a carbon fiber post. In this work the mechanical response to external applied loads is simulated by finite element analysis. Mechanical data obtained by some prototypes fabricated in the laboratory are used in the finite element model. Simulating various loading conditions, the resulting stress components are obtained and compared with those obtained of a natural tooth in laboratory experiments. It was found that the carbon fiber post showed the lowest peak stress inside the root and it also displayed a stress field very similar to that of a natural tooth.

The orthopedic profession has also benefited from the use of finite element analysis. Silva [2] demonstrated the effect of investigating the mechanics of skeletal fractures through finite element analysis. In order to predict fracture loads and fracture patterns for bone structures, sections of human vertebrate were loaded to failure. The finite element models were then analyzed under matching conditions. The finite element models provided predictions of yield load that were strongly correlated with experimental measured values. Comparisons between regions of observed fracture and of high predicted strain indicated that strain was an accurate indicator of the pattern of local fracture. It was concluded that finite element analysis can be used successfully to predict both global and local failure behavior of simplified skeletal structures.

The automotive industry has been able to use finite element analysis as a means to predict fatigue in commercial vehicles. Welded joints of the floor structure of city buses have been examined numerically and experimentally under bending and constant amplitude loading [3]. In this analysis, hot spot stresses at failure critical locations were calculated. The corresponding fatigue lives were determined experimentally. Overall

there was good agreement between calculated and experimentally determined critical locations.

Fatigue is an important failure mode for any structure that is subject to vibration and/or oscillatory loading. Suspension bridges are one such structure that is subject to fatigue. However, large suspension bridges have so many components that it would be difficult to analyze their fatigue damage using experimental measurement methods. Chan [4] was successful in showing finite element analysis is a feasible method of studying fatigue damage in large suspension bridges. The verification of the model was carried out with the help of the measured bridge modal characteristics and data measured by the structural health monitoring system installed on the bridge. Structural analysis using the finite element model is used to determine the components of the nominal stress generated by railway loadings and some typical highway loadings. The critical locations in the bridge span were identified with the results of the finite element stress analysis. The hot spot in a typical weld connection was also identified in the analysis. These results provided a basis for evaluating fatigue damage and predicted the remaining life of the bridge.

The use of finite element analysis and fatigue life determination is utilized extensively in the aircraft industry. Fixed wing aircraft and rotorcraft manufactures realizing the structural and economical impact of having a reliable and cost effective product goes without saying. With the cost of raw materials and labor constantly increasing, it is critical for aircraft manufactures to have the most optimal design possible. One of the highest recurring costs associated with an aircraft is part

replacement. Otherwise known as component retirement time (CRT), part replacement is entirely based upon how many flight hours a particular part is good for. It is common practice to determine the fatigue life of aircraft parts by full scale component testing. Most of the time, this is a very time consuming and costly process. Multiple test parts are required to obtain data that will give repeatable and consistent results. Material properties of the parts must be consistent in order to substantiate the validity of the test data.

Performing a fatigue analysis on helicopter components using finite element analysis is quite common. Schaff [5] did such an analysis on a helicopter tail rotor spar. The tail rotor spar was modeled by the finite element program using a composite layered shell element where laminate stiffness properties and strength properties were used. He employed a residual strength relation which assumes that the strength is initially equal to the static strength and decreases monotonically until failure, where failure is defined by a maximum stress failure criterion. The residual strength and fatigue relations results are compared to the failure criterion and damaged regions are degraded by adjusting the finite element stiffness matrix.

Damage caused by fatigue has several contributing factors which could be loads, design, material flaws, and manufacturing defects to name a few. But there are cases where part failure can occur due to a severe instantaneous event. Even in extreme situations as these, finite element analysis can be useful. Colombo [6] was able to determine the fatigue life of a helicopter tail rotor transmission that was subject to ballistic damage through the use of finite element analysis. The situation studied

involved a helicopter performing an emergency maneuver and a 30 minute return flight after the impact of a ballistic projectile on the shaft of the tail rotor transmission. A finite element model was used to simulate the impact of the projectile on the shaft. The model was also used to simulate the propagation of the crack caused by the impact of the projectile. Through this finite element method, it was then possible to determine the time required to reach failure of the shaft.

CHAPTER 3

METHODOLOGY

3.1 Main Rotor Parts Configuration and Description

The major main rotor components that have a direct impact in the evaluation process of this thesis are shown in Figure 3.1.

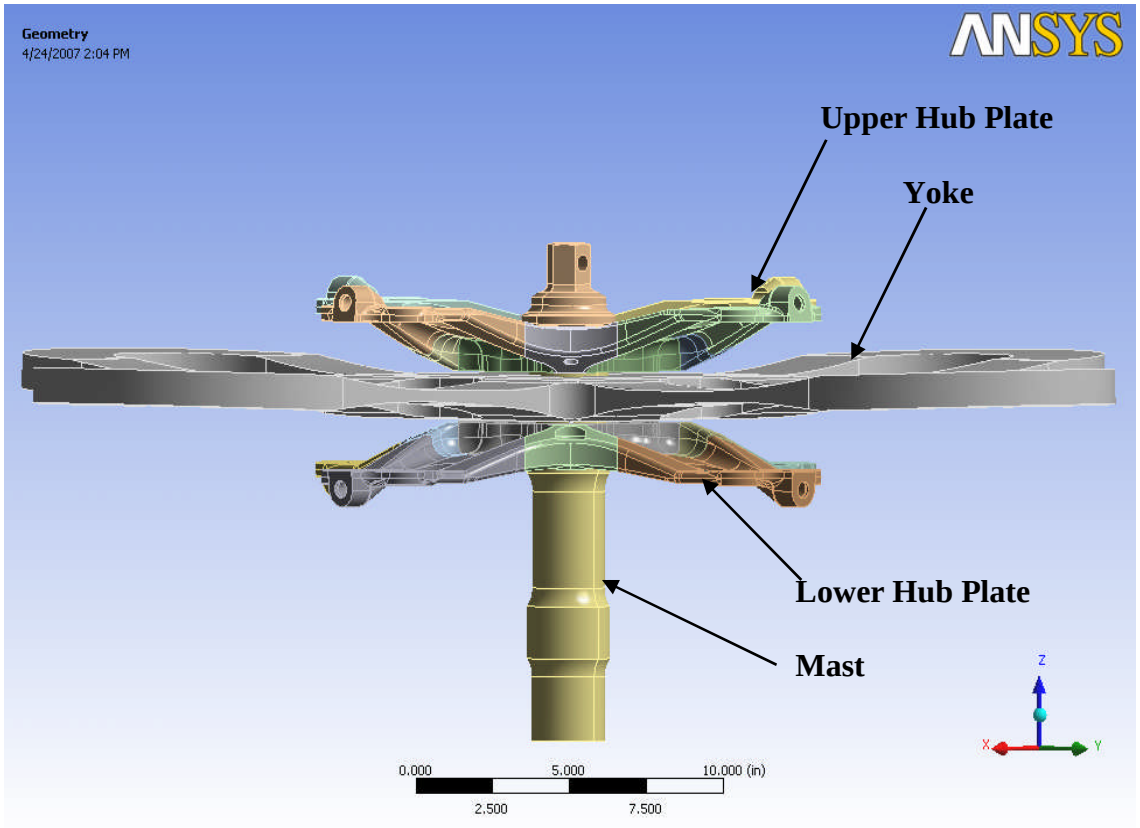

Figure 3.1 Main Rotor Components

The mast is 2.75” in diameter and 22” in length. The upper and lower hub plate is 1.75” thick, 20” in length and can be seen in detail on part drawing 0410-11058 and 0410-11059 respectively. The yoke is 1.5” thick and 60” in length. The lower cone seat is 5.75” in diameter and 6” in length. The geometry used for the finite element analysis is shown in Figure 3.2. The main rotor system is composed of four blades and each hub plate has the same corresponding number of arms. This helicopter is equipped with a fully articulated rotor system [7]. The fully articulated rotor system allows each blade to flap (move up and down out of plane), lead and lag (move back and forth in plane), and to feather or pitch (rotate about the pitch axis) independent of the other blades. Pitch change is the only action controlled directly by the pilot. The flapping and lead-lag occur as a natural function of pitch change and forces incurred during rotor operation. Therefore, the loads seen by each blade will only have direct impact on the corresponding arm of the upper and lower hub plate. In order to maximize the efficiency of the finite element model, only 1 arm of the upper and lower hub plate is utilized in the analysis. This approach will reduce the computer run time while still achieving the necessary accurate and reliable results.

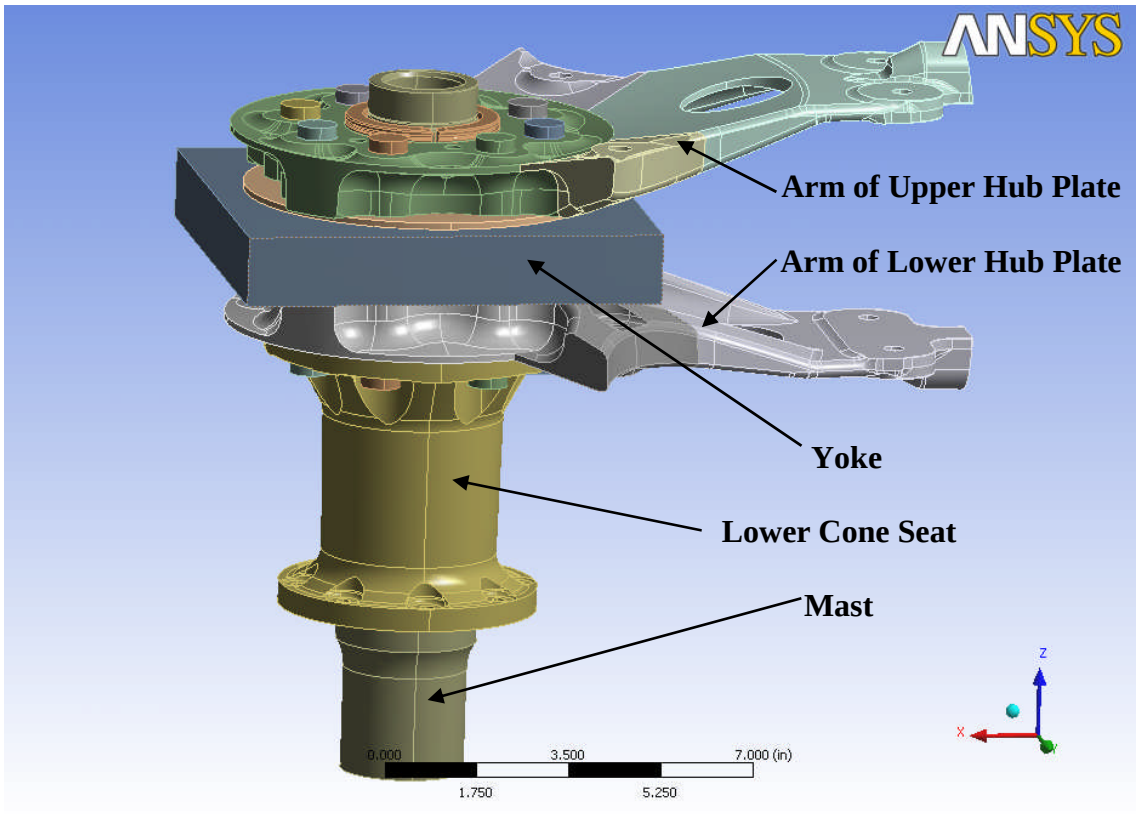

Figure 3.2 Components used for finite element analysis

3.2 Finite Element Approach

The finite element analysis was conducted by the use of the software program ANSYS [8]. The model contains an assembly of the mast nut, the upper and lower cones, the upper and lower hub plates, the lower cone seat, the yoke, hub bolts, and the mast. At the part interfaces, frictional contact elements were created, and a 0.05 coefficient of friction was assumed for this analysis. Only the inboard section of the

yoke was modeled in order to simplify the model to ensure the correct bolt clamp-up was simulated at the hub joint. The finite element model was meshed using a combination of tetrahedron elements and brick elements. There are 130,199 nodes which gives 390,597 degrees of freedom. Figure 3.3 shows the mesh of the complete finite element model. The mesh density was determined based upon part relevance in the stress analysis. The emphasis of this project was on the upper and lower hub plates. Therefore a large amount of time was spent on obtaining a finer mesh on the components in areas where stress concentrations were likely to be high. Some of the areas on the finite element model where mesh density was increased are fillets, radii, contour surfaces, and holes. These sections in general tend to have the highest stress concentration. Having a finer mesh in these areas helps to ensure that smooth stress distributions and accurate results are obtained. The mesh density process was repeated for several iterations before an optimal pattern was determined. The mesh density was experimented with until increasing the number of elements had minimal impact on the variation of the obtained stress values while at the same time not significantly increasing the running time of the analysis. Figure 3.4 illustrates an example of higher mesh density around holes in the lower hub plate.

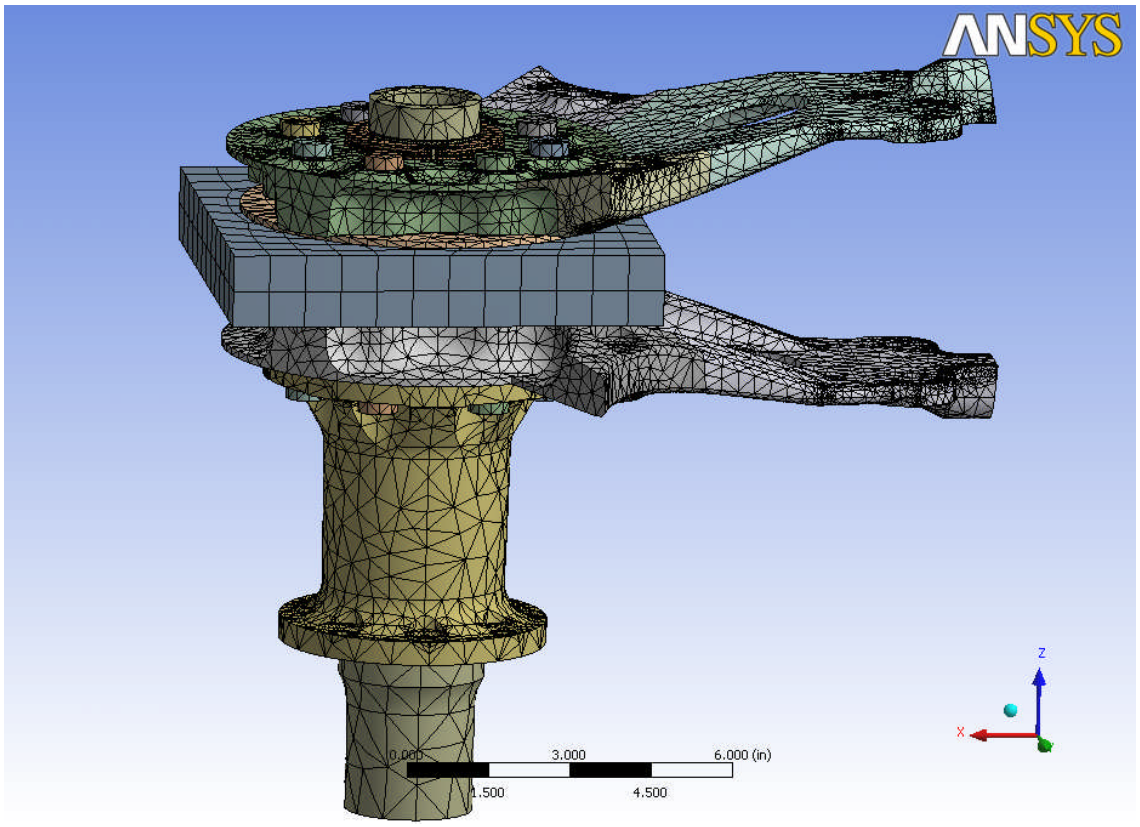

Figure 3.3 Complete mesh of finite element model

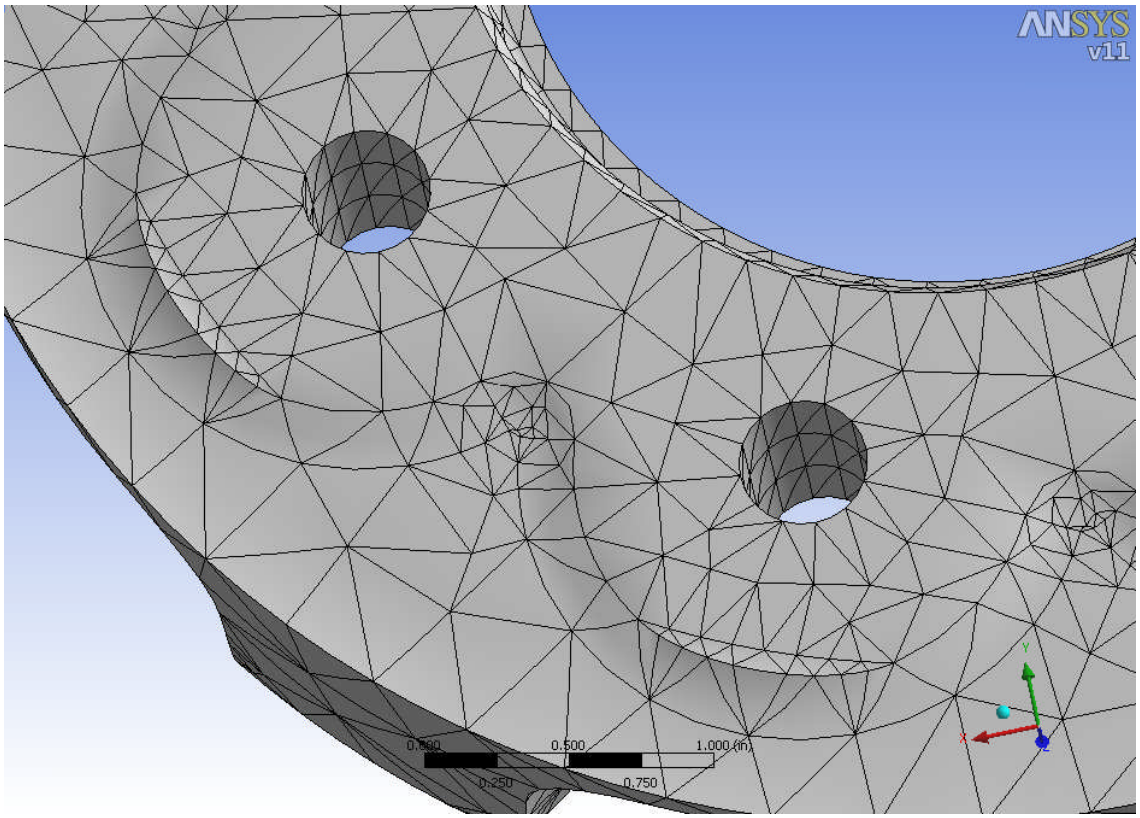

Figure 3.4 Example of higher mesh density

3.3 Miner's Rule

The fatigue life calculation in this research will be accomplished through a process called Miner's Rule [9]. This method may be used to approximate the cumulative fatigue damage at a point in a metallic part from the repeated exposure to cycles of various stress levels. For a given maximum and minimum stress levels, the fatigue life in terms of the number of cycles is found from a stress vs number of cycles (S/N) curve. Miner's rule also postulates that the fractional fatigue damage from each of a succession of different loading conditions adds together linearly and that crack

initiation occurs when the sum of the damage fractions reaches 1.0 [10]. The linear assumption essentially means that the fatigue damage from each load cycle is an independent event, not affected by what has happened before or the current state of damage on the component. The fatigue damage resulting from exposure to a given stress level is proportional to the number of applied cycles (n) at that stress level divided by the allowable number of cycles (N) to fracture at that same stress level found from the component S/N curve. This ratio (n/N) is the ratio of applied cycles to the allowable cycles and is used to measure the incremental fatigue damage. If several levels of stress amplitudes are applied, the total damage is the sum of the individual damage ratios:

$$Total\ Damage = \Sigma\ (n_i / N_i) \tag{3.1}$$

Fracture is assumed to occur when the sum of the individual damage ratios equals 1.0. It is necessary to note that Miner's Rule is used by helicopter manufactures world-wide to determine safe life retirement times, and probably 95% of the fatigue loaded parts now in service were substantiated using Miner's Rule. It is also important to note the use of Miner's Rule is not to predict a time to failure, rather it is used to estimate a safe life retirement time. This is the critical justification for the use of Miner's Rule in helicopter fatigue substantiation.

Miner's Rule will be used in conjunction with S/N curves in approximating the fatigue life of the hub plates being analyzed. The fact that Miner's Rule is entirely

empirical does not detract from its validity. Experience has shown in full scale test or in service, where Miner's Rule was found to be a contributor to premature cracking [10]. This experience is true for all of the other American and European helicopter manufactures as well, and covers more than fifty years of experience with more than a million safe-life parts. Overall it is safe to say that Miner's Rule is an appropriate and sufficient methodology for safe life fatigue substantiations for the materials being used and the stress levels for which they are designed and operate.

3.4 Loading and Boundary Conditions

In the finite element model the mast is fixed at the base as shown in Figure 3.5 to prevent rigid body motion in the *x*, *y*, and *z* directions. The lower cone seat is also constrained in a similar manner as the mast. Pretension elements are used to simulate the pretension load through the bolts due to the bolt torque-up. These loads are shown in Figure 3.6. The loading in the model is achieved in a three step process. Load step 1 is the bolt preload on the eight main bolts which hold the upper and lower hub plates together. Load step 2 is the load from the torque-up of the main rotor mast nut. Load step 3 is the shear bearing chord and shear bearing beam loads encountered during flight conditions. The maximum peak load and minimum peak load were applied to the model for each flight condition. For clarification, the maximum and minimum designations for the load values refer to the largest positive and the largest negative values respectively. The maximum and minimum load cases were applied to the upper and lower hub plates

at the connection point where an elastomeric bearing is assembled between the upper and lower hub plates as shown in Figure 3.7.

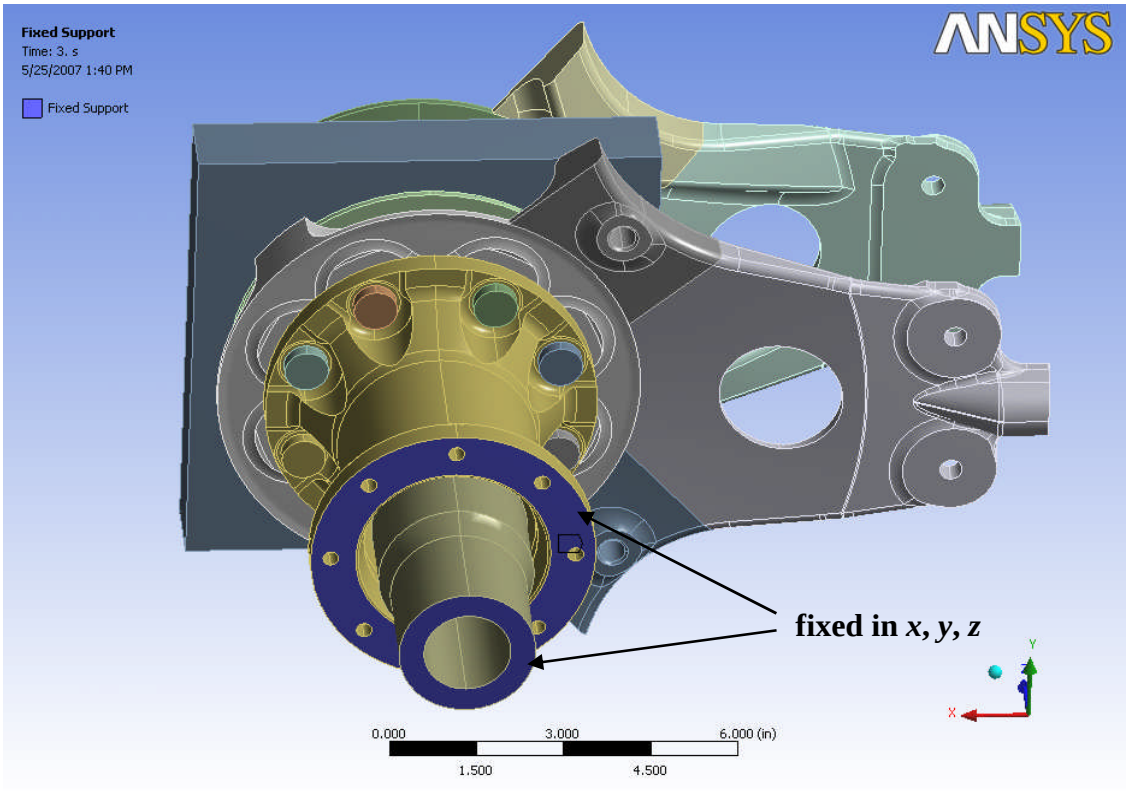

Figure 3.5 Fixed Support Boundary Conditions

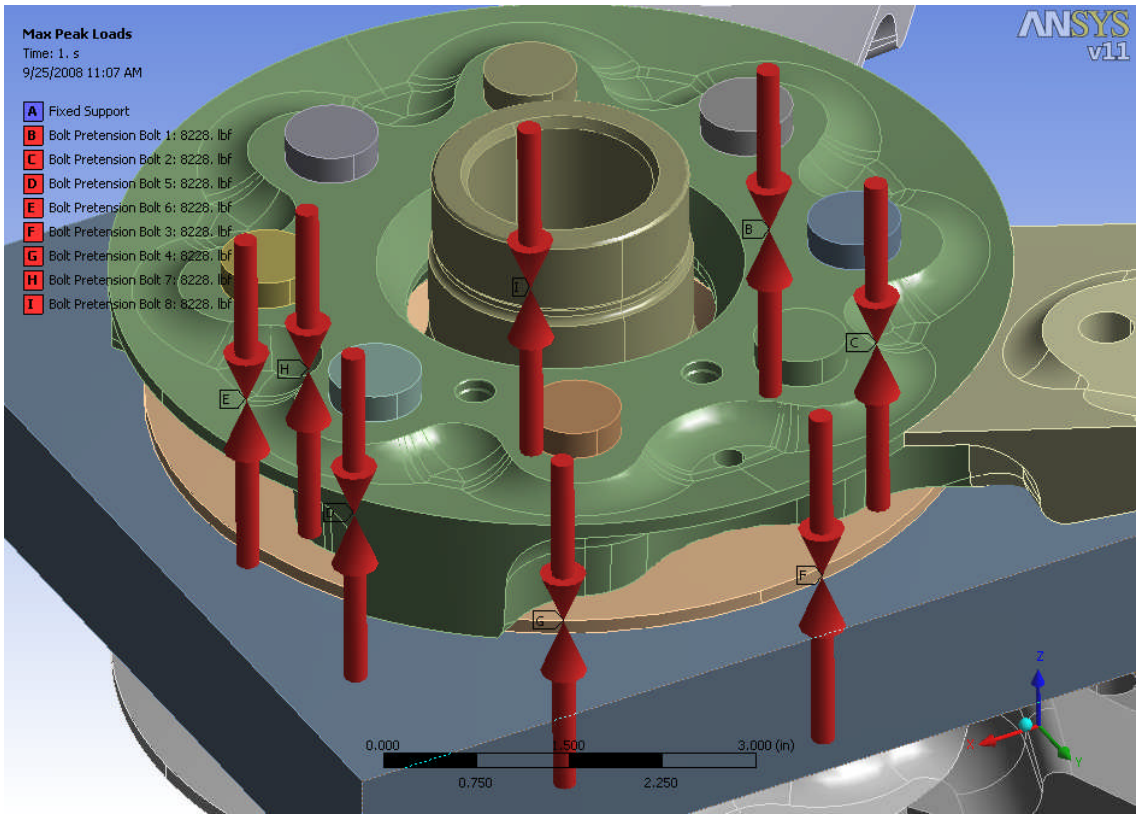

Figure 3.6 Bolt Preload on Hub Plate Bolts

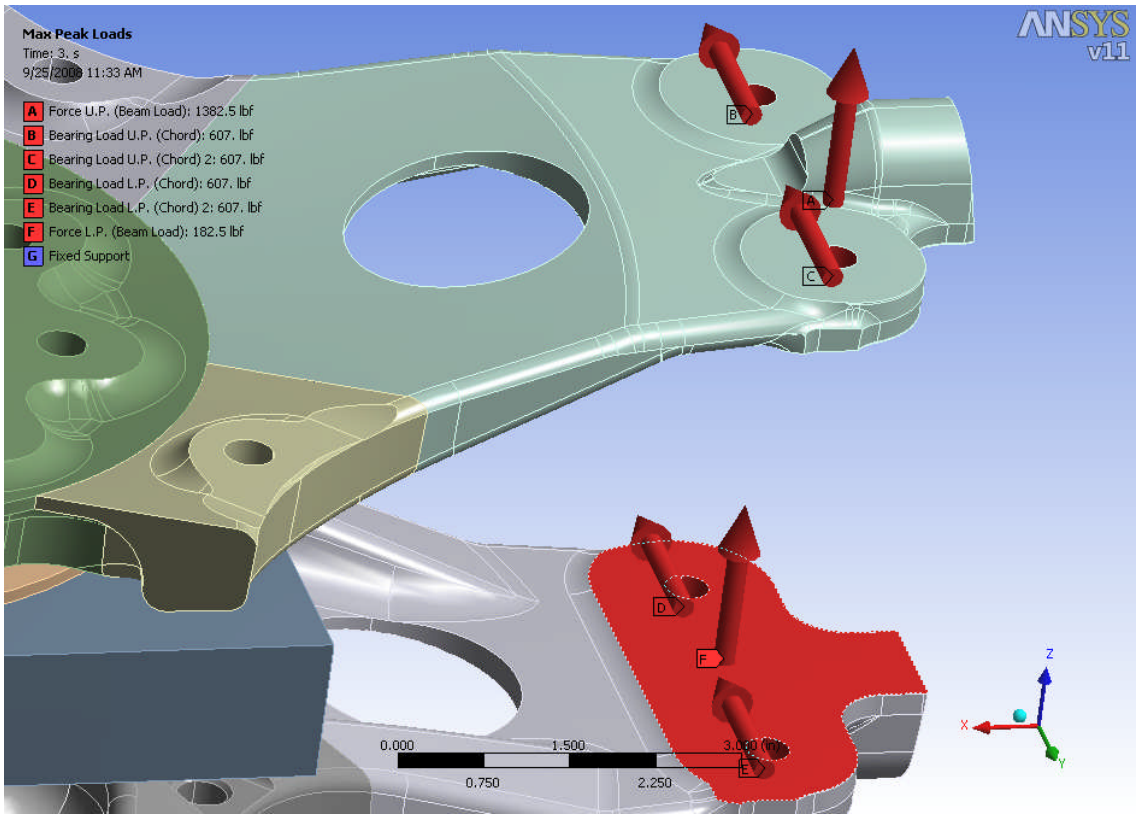

Figure 3.7 Applied Beam and Chord Loads on Hub Plates

The sign convention for the main rotor follows a "right-hand rule." Each arm of the hub plate has a local coordinate system that remains fixed in relation to the individual arms, independent of the hub location around the mast. The positive *x*-axis runs span-wise along the length of the blade, pointing away from the hub, towards the blade tip. The positive *y*-axis points towards the leading edge of the blade. The positive *z*-axis points towards the upper airfoil surface of the blade, or in other words, towards the top portion of the mast. We will refer to loads applied in the *z* direction as beam loads and loads applied in the *y* direction as chord loads. Therefore, positive thrust puts

the mast in tension and forces the main rotor to turn counter-clockwise when looking at the aircraft from above.

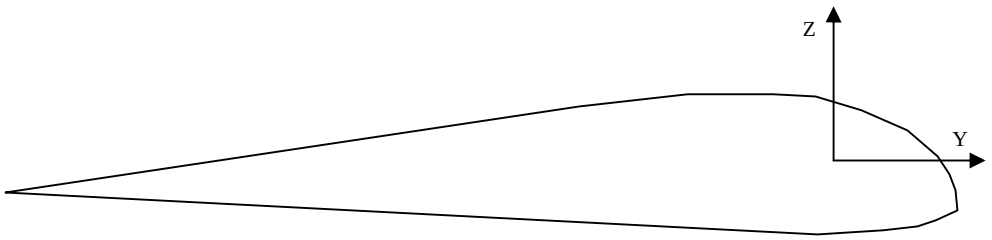

Figure 3.8 Sign Convention of Blade Cross Section

In determining the preload on the main bolts that hold the hub plates together, the following equation is used,

$$F = 5 * T / d \qquad (3.2)$$

where T is the recommended torque value based on bolt size and d is the bolt diameter [11].

In order to determine the fatigue life of a component, three basic factors must be known. These are (1) knowledge of the fatigue strength (endurance strength) of the material, (2) the magnitude of the applied loads, and (3) the frequency of occurrence of these loads in normal operation [11]. When the measured flight loads produce stresses greater than the endurance strength of a component, Miner's cumulative damage method is used to calculate the fatigue life taking into consideration the frequency of occurrence of each flight condition. Using the maximum peak and minimum peak values from the measured flight loads applied to the finite element model, we will

investigate two different load cases. The first load case is the maximum peak and minimum peak load that are seen during high cycle or 1 per revolution flight conditions. These loads are used in determining the fatigue damage due to high cycle fatigue (HCF) stress. The fatigue damage from high cycle stress is calculated and based upon the revolutions per minute of the rotor system and the current calculated retirement time of the component.

The second load case will be to apply the maximum peak and minimum peak load from low cycle or ground-air-ground (GAG) cycles. One complete GAG cycle is the time from when the aircraft is sitting on the ground, and then performs take-off and flight maneuvers, and then back on the ground with engine turned off. These loads are used in determining the fatigue damage due to low cycle fatigue (LCF) stress. The fatigue damage from low cycle stress is calculated and based upon the number of occurrences of that particular flight maneuver. In determining which flight maneuver loads to use in the fatigue analysis, most of the time there will be a certain flight maneuvers in the total flight regime that stand out among all the rest. When the worst case flight maneuver is not so easily identifiable, it may be necessary to consider multiple maneuvers in the fatigue analysis. For this research we do have two specific flight maneuvers that demonstrated maximum and minimum peak loads that were considerably higher than all others in the flight regime.

Once the stress values are obtained from the maximum peak and minimum peak load conditions, the steady stress and oscillatory stress values are calculated by performing a solution combination function in ANSYS. Steady stress is calculated by

adding the maximum peak stress value with the minimum peak stress value then dividing by two. Oscillatory stress is calculated by subtracting the minimum peak stress value from the maximum peak stress value then divide by two. When selecting the numerical stress values from the maximum peak and minimum peak results, it is critical that the same location on the component being evaluated is chosen for each case. Otherwise the fatigue process evaluation will not be valid. This will be clarified later in the thesis.

The maximum peak and minimum peak loads in this project are from 1 per revolution and (GAG) cycles. Depending on the configuration of the rotor system, either condition can be a major contributor to fatigue damage in the outboard regions of the hub. During the part design phase, limit load conditions would also need to be considered as well. Limit load conditions will not be considered as part of this project since the focus of the project is to determine an appropriate fatigue life for the components being evaluated. The contributing factors that will be taken into consideration for this project are all fatigue related. Two types of fatigue damage were analyzed from the different loading conditions. They are low cycle fatigue such as GAG loads and high cycle fatigue such as one occurrence per rotor revolution. The sum of the damage caused by low cycle and high cycle fatigue will used to calculate Miner's cumulative damage. This in turn will then dictate the appropriate safe life flight hours for the component and also establish a high probability in which initiation of component failure can be reduced.

CHAPTER 4

RESULTS

The loads that are applied to the finite element model are listed in Table 4.1. The results from load case 1 will be used to calculate the fatigue damage caused from high cycle stress. The results from load case 2 will be used to calculate the fatigue damage caused from low cycle stress.

Table 4.1 Load Data Summary

Loading	Load Direction	Load Case 1 Max Peak	Load Case 1 Min Peak	Load Case 2 Max Peak	Load Case 2 Min Peak
Beam Shear (lbs)	Z	1565	-1364	600	-329
Chord Shear (lbs)	Y	2426	-2077	1807	-1642

To support the fatigue evaluations, a stress spectrum is developed for a selected location on the structural component. The local stress spectrum is needed to estimate the crack initiation time (CIT) as the basis for establishing the component retirement time (CRT). Component reference stresses are established for each load case listed above. The steady and oscillatory stress values for each load case were obtained by utilizing a solution combination function in ANSYS. This function allows one to select multiple load cases and combine them as necessary based on the application which is being investigated. The steady stress values for each load case were obtained by combining the corresponding maximum peak and minimum peak load cases. A factor of 0.5 was

applied to the maximum peak and minimum peak results, which in turn gives the steady stress values for that load case. The oscillatory stress values for each load case are obtained in a similar fashion, except a factor of 0.5 is used for the maximum peak results and a factor of -0.5 is used for the minimum peak results. Mathematically the steady and oscillatory stress values are calculated by the formula shown below.

$$\sigma_{steady} = 0.5\,(\sigma_{max\_peak} + \sigma_{min\_peak}) \tag{4.1}$$

$$\sigma_{oscillatory} = 0.5\,(\sigma_{max\_peak} - \sigma_{min\_peak}) \tag{4.2}$$

At this juncture it would be prudent to determine if the finite element analysis is accurately representing the main rotor system components that are represented in the model under the applied loads. One way to accomplish this is to compare the measured flight data of a fixed reference point to that of one from the finite element analysis. For this comparison we will use the measured flight data of the mast torque from load case 1 during maximum peak loading condition. The instrumentation on board recorded a mast torque value of 102,818 in-lbs. This data can be extracted from the ANSYS model by taking the moment reaction at the fixed boundary location of the center mast. This value is calculated to be 105,512 in-lbs. This indicates that the finite element model is within 2.62 percent of the actual measured flight data. Based on this comparison, it is safe to say the loads in Table 4.1 are properly applied to the finite element model and the analytical evaluation collaborates with our known flight data.

4.1 Upper Hub Plate Results

The high cycle steady and oscillatory stresses on the upper hub plate stem from maximum and minimum peak loads from load case 1. The worst location for steady and oscillatory stress combinations was determined and is presented below. This location was chosen from a visual inspection of the ANSYS output. It is important to note that once the region with the highest steady stress is determined, the same location or nodal point will be the reference point for the stress data for all load cases for that particular component. As stated earlier, this process must be followed in order to obtain accurate values for Miner's damage. The results for load case 1 for the upper hub plate show the highest steady stress value near the outboard edge of the hub plate. The region has a slight change in contour which would explain the high stress value in this region. The highest steady principal stress value is 19,930 psi which is seen in Figure 4.1. The corresponding oscillatory principal stress value for the same location is 7191 psi.

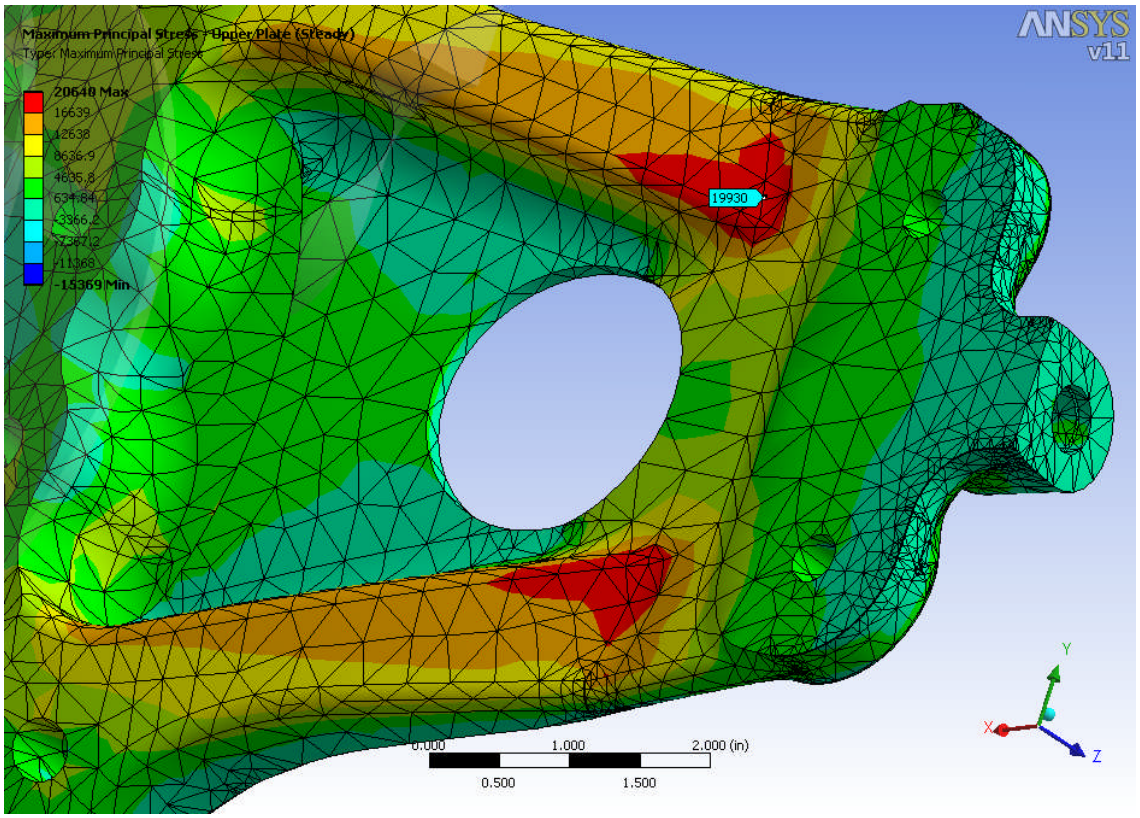

Figure 4.1 High Cycle Steady Stress (Load Case 1) – Upper Hub Plate

The low cycle steady and oscillatory stresses on the upper hub plate stem from maximum and minimum peak loads from load case 2. The same location for steady and oscillatory stress combinations on the upper hub plate was selected for load case 2 as was used in load case 1 and is presented below. The highest steady principal stress value is 20,943 psi which is seen in Figure 4.2. The corresponding oscillatory principal stress value for the same location is 12,362 psi and is shown in Figure 4.3.

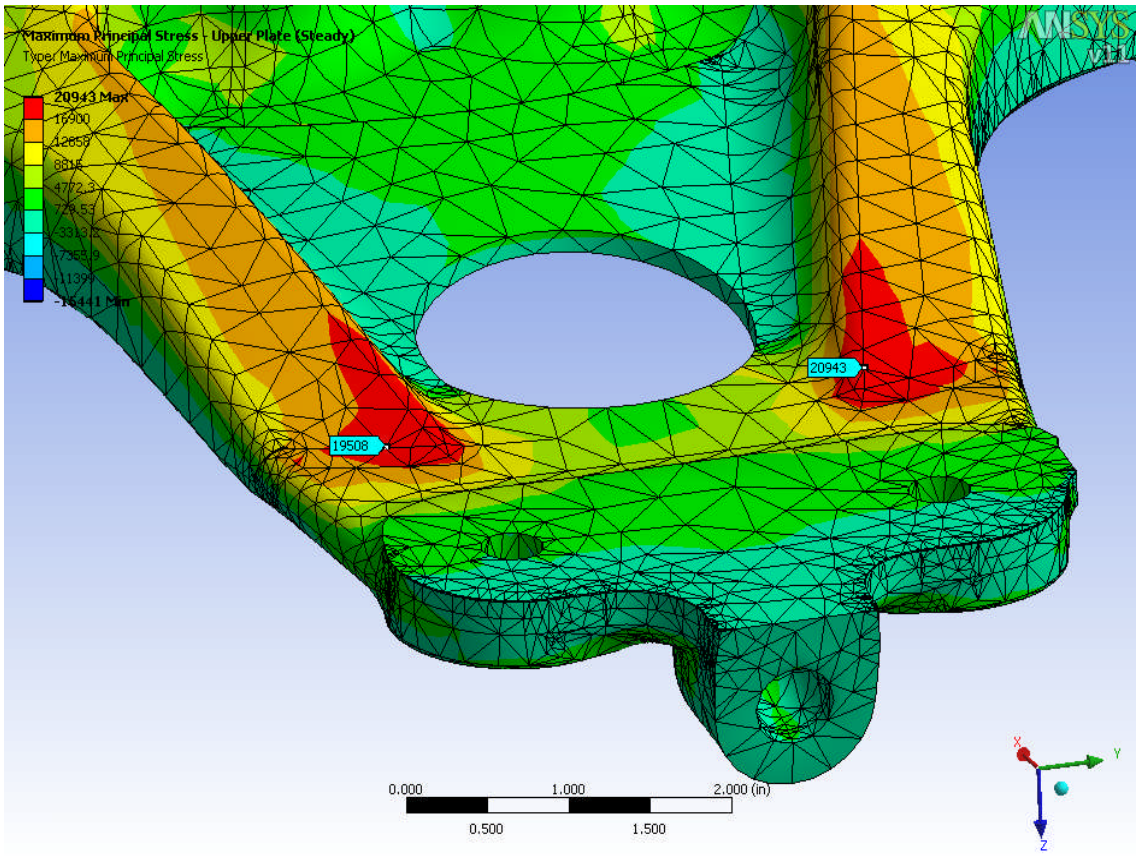

Figure 4.2 Low Cycle Steady Stress (Load Case 2) – Upper Hub Plate

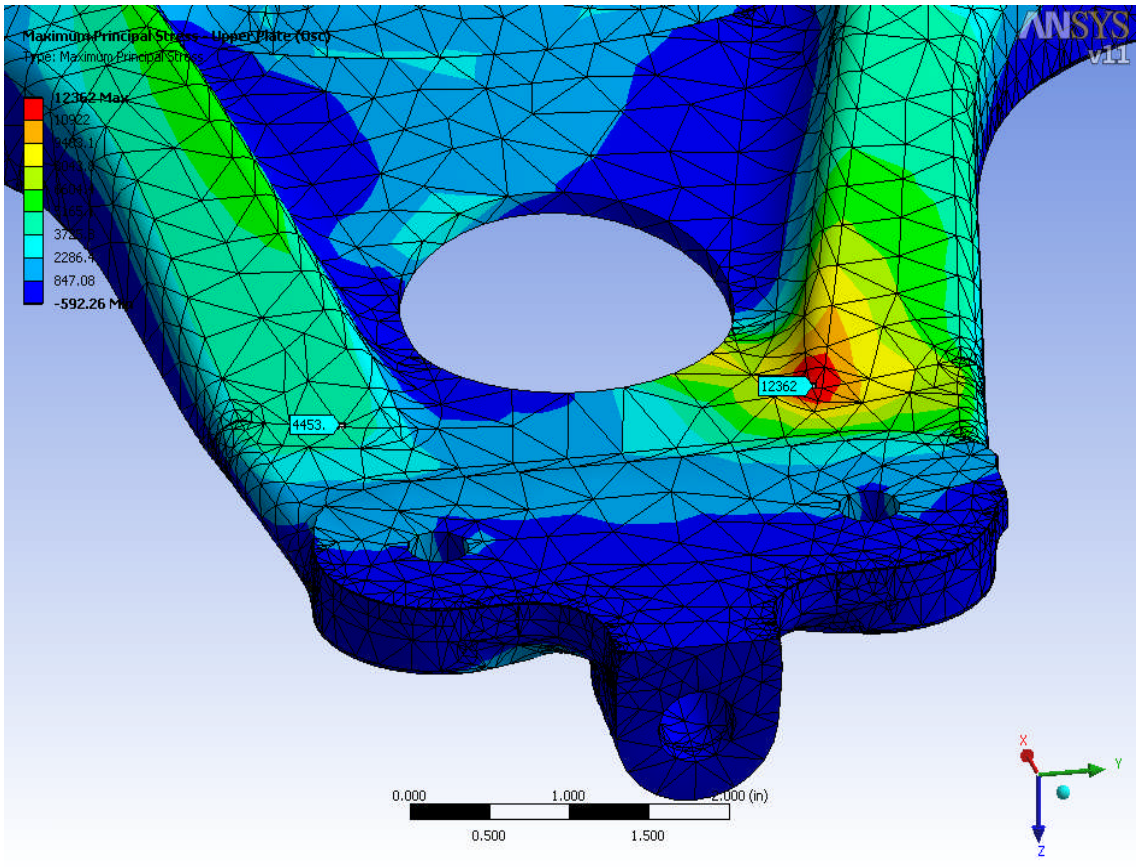

Figure 4.3 Low Cycle Oscillatory Stress (Load Case 2) – Upper Hub Plate

4.2 Lower Hub Plate Results

The high cycle steady and oscillatory stresses on the lower hub plate stem from maximum and minimum peak loads from load case 1. Similar to the upper hub plate, the worst location for steady and oscillatory stress combinations on the lower hub plate was selected from a visual inspection of the ANSYS output and is presented below. The results for load case 1 for the lower hub plate show the highest steady principal stress value near the outboard edge of the hub plate. The region has a slight change in contour

which would explain the high stress value in this region. The highest steady principal stress value is 19,170 psi which is seen in Figure 4.4. The corresponding oscillatory principal stress value for the same location is 7311 psi.

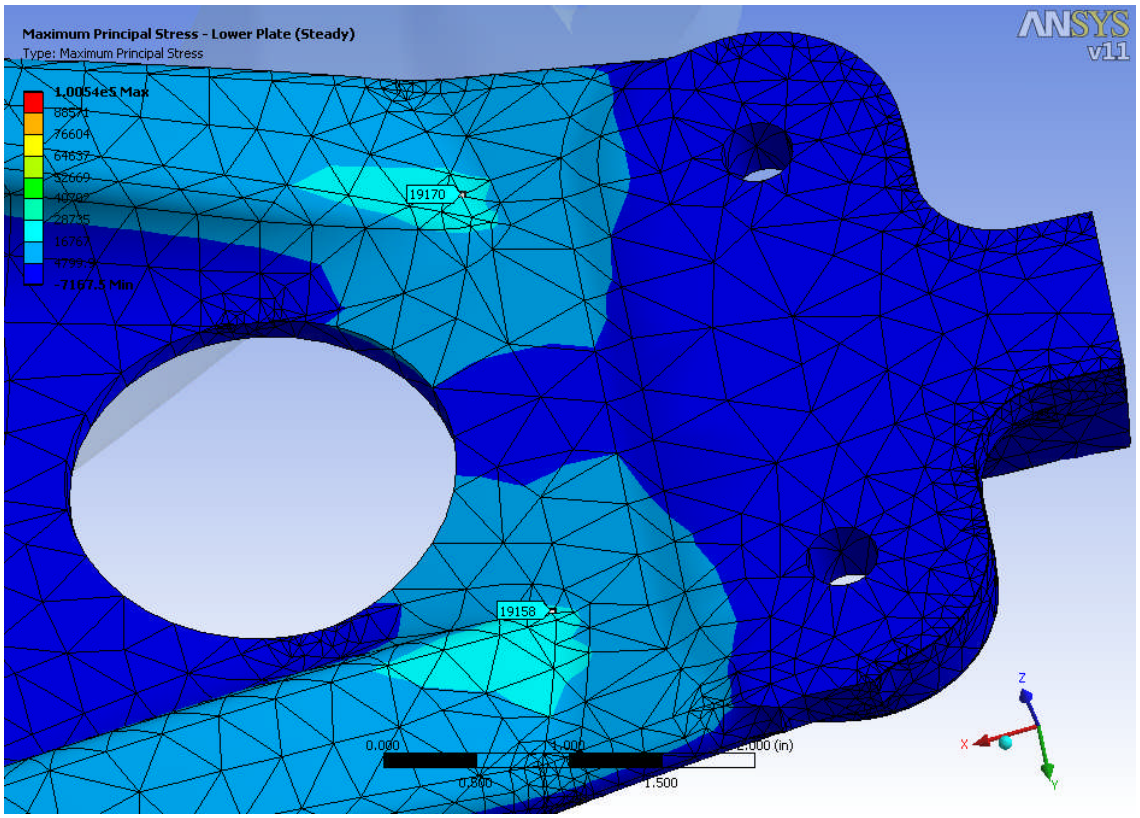

Figure 4.4 High Cycle Steady Stress (Load Case 1) – Lower Hub Plate

The low cycle steady and oscillatory stresses on the lower hub plate stem from maximum and minimum peak loads from load case 2. The same location for steady and oscillatory stress combinations on the lower hub plate was selected for load case 2 as was used in load case 1 and is presented below. The highest steady principal stress

value is 18,730 psi which is seen in Figure 4.5. The corresponding oscillatory principal stress value for the same location is 11,865 psi and is shown in Figure 4.6.

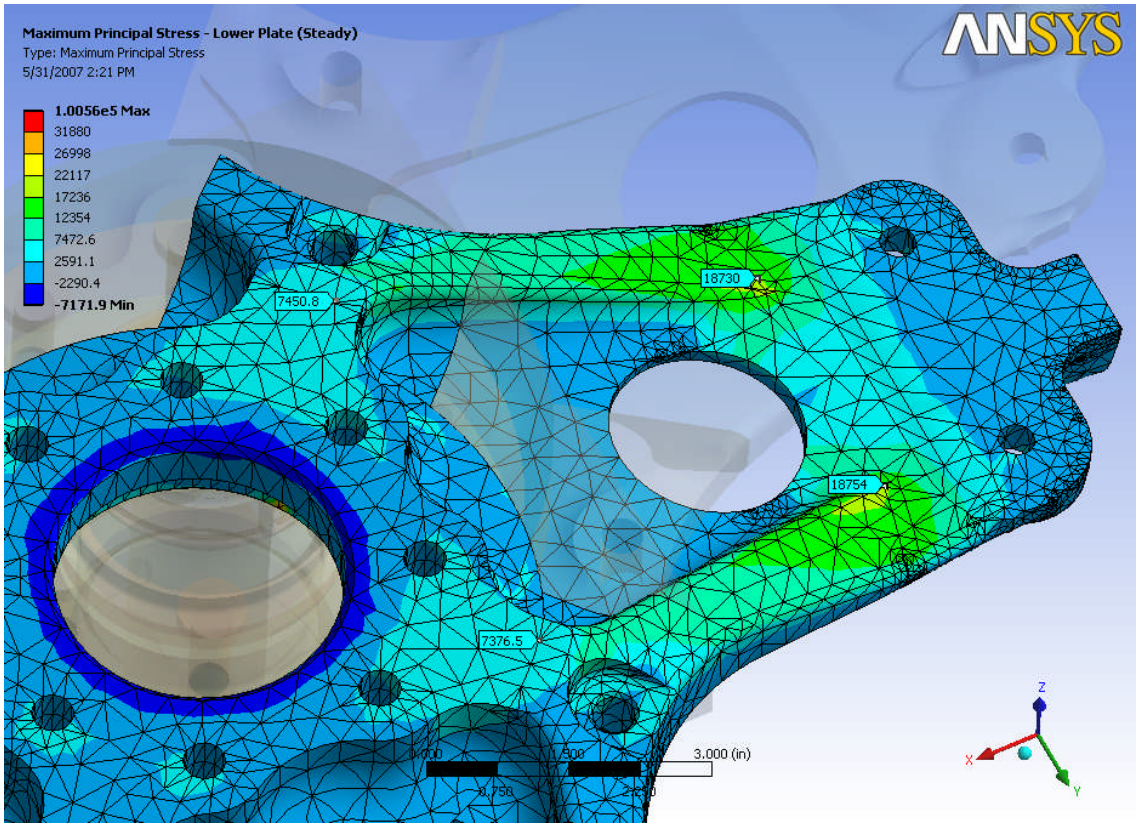

Figure 4.5 Low Cycle Steady Stress (Load Case 2) – Lower Hub Plate

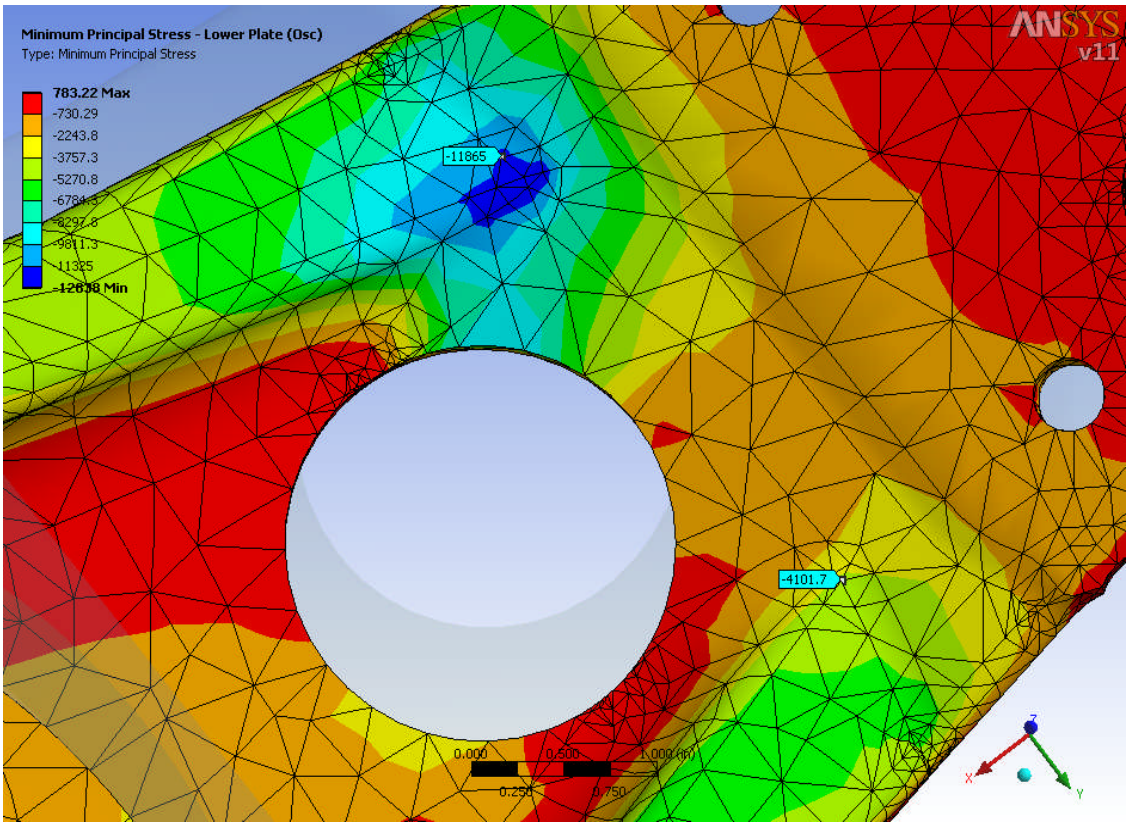

Figure 4.6 Low Cycle Oscillatory Stress (Load Case 2) – Lower Hub Plate

As we can see from the stress values obtained from the finite element model, the highest steady and oscillatory stress locations are located relatively in the same location, outboard portion of the hub, for both the upper and lower hub plate. This is not surprising seeing how the upper and lower hub plates have the same shape and contour in this region. The upper and lower plates do differ at the inboard portion of the part. This difference is primarily for manufacturing and assembly quality control. A

summary of highest fatigue stresses for all load cases at the locations indicated in the figures is given in Table 4.2.

Table 4.2 Summary of Fatigue Stresses

	High Cycle (1/rev)		Low Cycle (GAG)	
	Steady (psi)	Osc (psi)	Steady (psi)	Osc (psi)
Upper Hub Plate	19930	7191	20943	12362
Lower Hub Plate	19170	7311	18730	11865

Besides the locations used to obtain the worst fatigue stress for the hub plates, multiple locations where also chosen to collect data points to get a comparison of stress values on the hub plates. These stress values are plotted on a Soderberg diagram which will indicate where the data points fall in regards to the allowable fatigue life of the hub plates. The various stress data points are indicated in Figure 4.7. In examining the Soderberg diagram, the region under the solid blue line indicates any data points in this region would show that a component would have unlimited fatigue life. Unlimited fatigue life is in reference to the total life of the aircraft. In other words, the component would never have to be replaced for the life of the aircraft as long as the steady and oscillatory stresses are within this region for the component in question. As we can see from the graph, there are two data points which are above the constant fatigue life line. Not only are the data points above the constant fatigue life line, they are also in close proximity to another reference line on the graph, the solid green line which represents a safe life CRT of 240,000 cycles. The line was arbitrarily chosen to give an

approximation of the number of allowable cycles the hub plates can encounter under the applied load conditions.

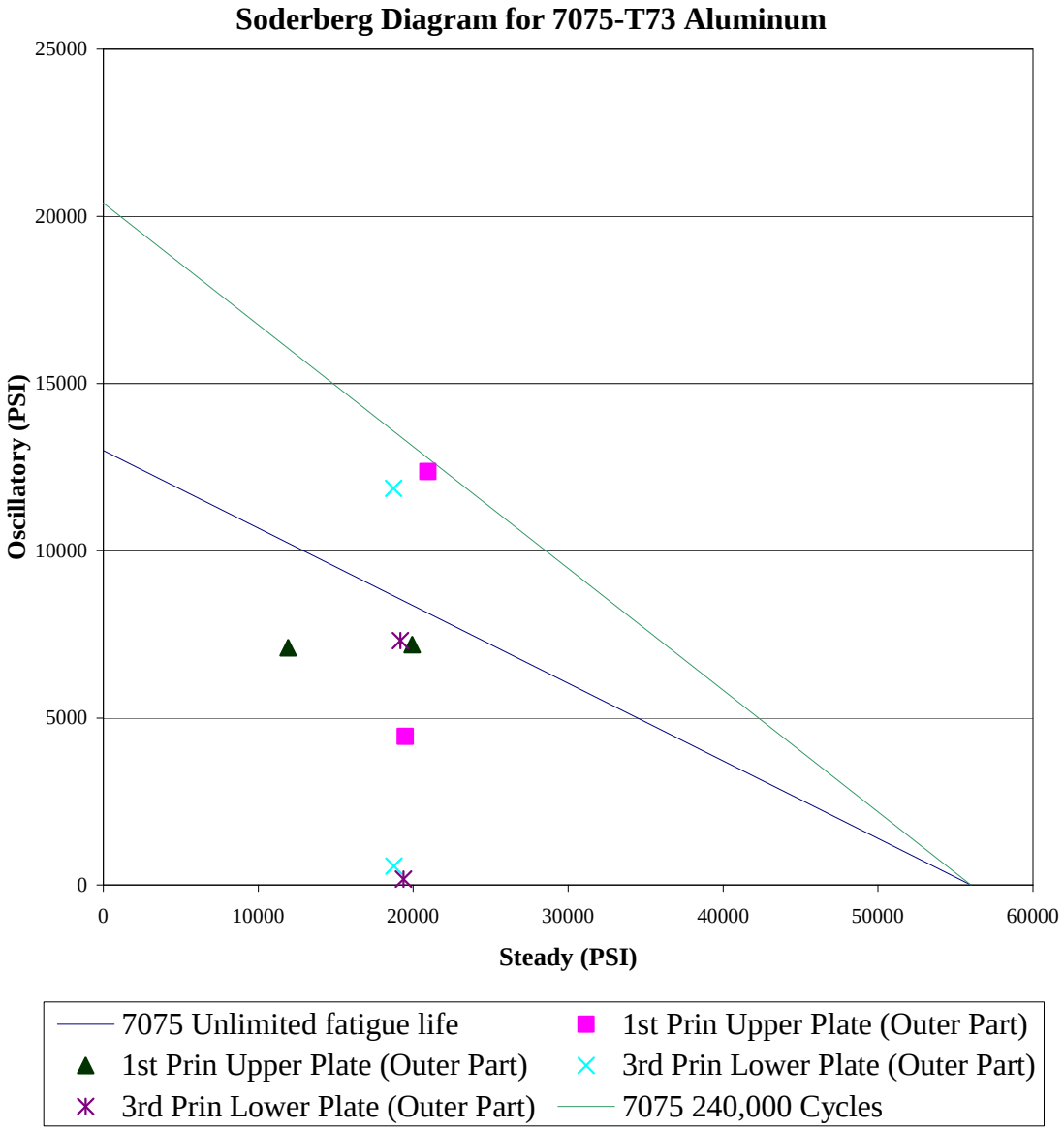

Figure 4.7 Soderberg Diagram for Upper and Lower Hub Plates

This may seem trivial to even have this diagram since we already know the published CRT of the hub plates to be 2500 hours. This diagram serves a twofold purpose. First, it validates the finite element model accuracy of representing the components of the main rotor system, especially the upper and lower hub plates. Second, the Soderberg diagram indicates that the hub plates do not have unlimited fatigue life for the total life of the aircraft and the allowable number of cycles should not be less than 240,000 cycles.

4.3 Derivation of S/N Curves

Small specimen stress life coupon test data will provide the basis for the determination of S/N curves. This data was generated by coupon testing using small specimens cycled under constant stress amplitude until fracture [12]. The effect of steady tensile stress will reduce the fatigue strength of the component and must be included in the fatigue evaluations. Plotting the fatigue test results for a range of steady stresses will produce lines of constant fatigue life. The constant life curves provide the relation between oscillatory stress amplitude versus steady stress for a fixed number of cycles to failure. Constant life curves have been widely used in aviation to estimate the effects of steady stress especially when available test data is limited to a few steady stress levels. The constant life fatigue diagram [12] that will be utilized for aluminum 7075-T73 is seen in Figure 4.8.

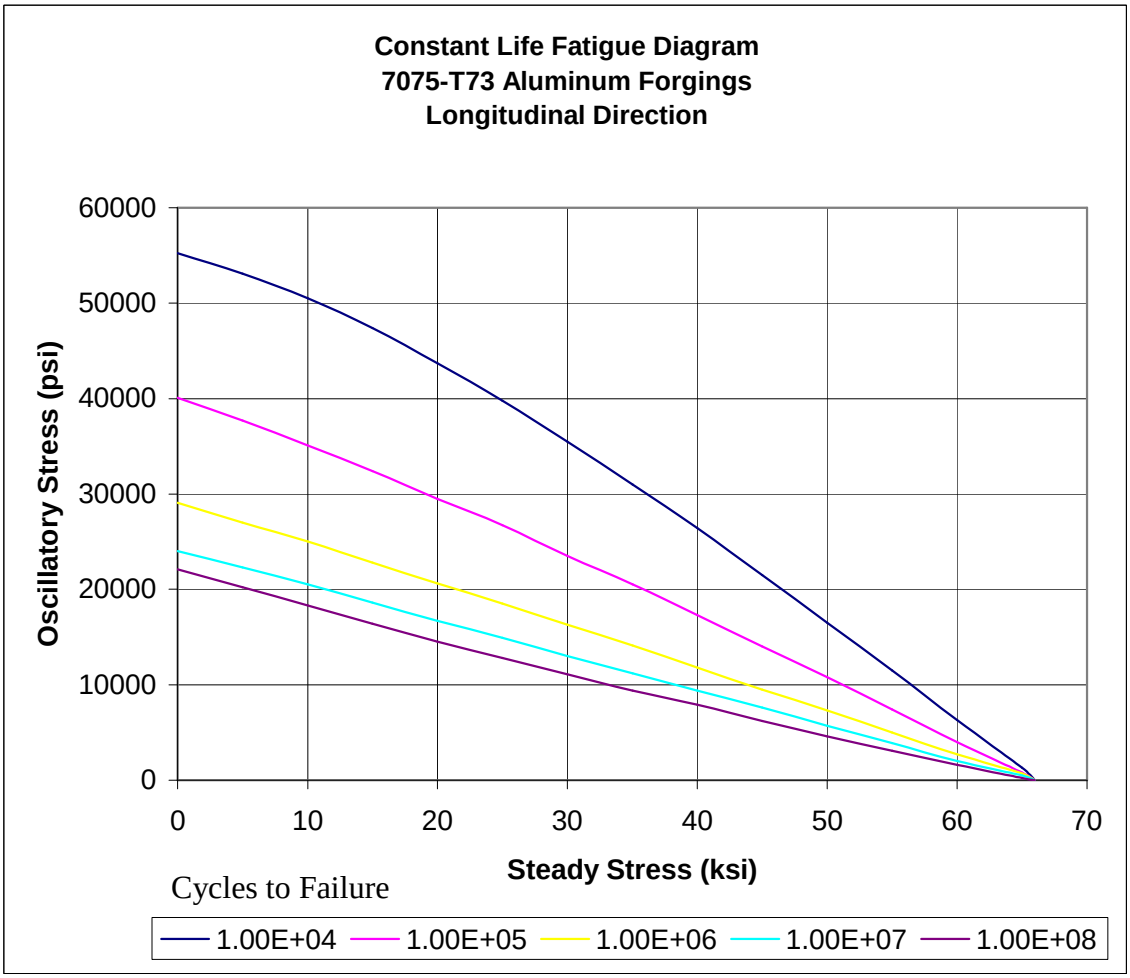

Figure 4.8 Aluminum 7075-T73 Constant Life Fatigue Diagram

When small specimen fatigue data is used as the basis for establishing the CIT of a component, the data must be adjusted in order to simulate the conditions present in the full scale structure. The crack initiation characteristics of a typical component depend on several factors such as local stress magnitude, volume of the material affected by the stress gradient, and the surface finish characteristics. Additional adjustments are made that account for scatter in the material fatigue strength in

combination with a life safety factor. The resulting S/N curve is termed the allowable curve that is used to establish the number of allowable cycles in order to calculate the fatigue damage for each regime in the flight spectrum.

The effect of a geometric stress concentration has a significant impact on the fatigue life in the region of the stress concentration relative to the surrounding regions. In general, the effect of component geometry on stress concentration is determined through the use of a finite element model. Therefore the finite element model already takes into account the stress concentration due to variations in geometry. The fatigue strength reduction from a stress concentration is primarily characterized by fatigue test data of notched specimens relative to un-notched specimens [13]. A fatigue notch factor can be established from this test data. Because a finite element model is used to establish stress values, the geometric stress concentration factor and fatigue notch factor will not be applied again in calculating the allowable fatigue strength of the hub plates since these factors are accounted for in the finite element analysis.

Surface roughness can also cause a reduction in fatigue life. The upper and lower hub plates are machined and shot peened during the manufacturing process. The purpose of shot peening metal parts is to induce residual compressive stresses in specified surfaces, for the purpose of improving resistance to fatigue, stress corrosion cracking, and galling [14]. The effect of the compressive stresses will slow down the process of crack initiation, thereby retarding fatigue cracks.

A size effect factor is also taken into account since experimental data indicates that fatigue strength is a function of specimen size. Fatigue crack initiation occurs at

specific weak spots intrinsic in normal material. The probability of having a weak spot is higher for a large volume of material than for a small volume.

Adjustments to the small specimen fatigue data include the effects of the local geometry, the manufacturing process, and the material reliability. The constant fatigue life fatigue diagram is used in conjunction with the fatigue reduction factors mentioned above to obtain the allowable oscillatory stress. The relationship between these factors is as follows:

$$S_o(a) = S_o * F_R * F_{SE} * K_t / (K_f * K_{SF}) \quad (4.3)$$

where the factors are: reliability factor (F_R), size effect factor (F_{SE}), geometric stress concentration (K_t), notch sensitivity factor (K_f), and surface finish factor (K_{SF}). The oscillatory stress (S_o) we extracted from the constant life fatigue diagram is multiplied by the reduction factors to obtain the allowable oscillatory ($S_o(a)$) stress value.

4.4 Miner's Damage Calculations for Upper Hub Plate

Now that we have our oscillatory stress values from the finite element analysis, we need to use these values to get the fatigue allowable stress values for the hub plates. The S/N curve for the upper hub plate from the high cycle fatigue (HCF) case will be established first. The steady stress value from the finite element model for this condition is 19,930 psi and the oscillatory stress value is 7191 psi. Taking the steady stress value, the corresponding oscillatory stress values are obtained from Figure 4.8 at each number of cycles shown on the graph. The reduction factors that are used in calculating the

allowable oscillatory stress value were derived from small specimen test samples and were chosen according to material alloy. Shown in Table 4.3 is the allowable S/N calculation for the upper hub plate for the high cycle fatigue case.

Table 4.3 Allowable S/N Calculation for Upper Hub Plate HCF

N(cycles)	Stress (Osc)	K_f	K_{SF}	K_t	F_R	F_{SE}	$S_o(a)$
10000	43700	1	1	1	0.61	0.8	21325.6
100000	29700	1	1	1	0.61	0.8	14493.6
1000000	20700	1	1	1	0.61	0.8	10101.6
10000000	16700	1	1	1	0.61	0.8	8149.6
100000000	14600	1	1	1	0.61	0.8	7124.8

The oscillatory stress of 7191 psi is between the fatigue allowable values of 8149.6 and 7124.8 psi. This indicates that for the high cycle fatigue case for the upper hub plate, the allowable number of cycles is between 10^7 and 10^8 cycles. Plotting the allowable oscillatory stress values versus the number of cycles, a corresponding S/N curve will give a graphical representation in which Miner's damage can be calculated for this particular location and load case. Figure 4.9 is the S/N allowable curve for the upper hub plate subject to high cycle fatigue loading. The oscillatory stress value of 7191 psi is indicated on the graph by a larger data point. This data point is calculated by generating a best fit curve between the data points for 10^7 and 10^8 cycles. This best fit curve gives an equation in which the allowable number of cycles can be calculated through a logarithmic linear interpolation. This equation is shown on the graph in Figure 4.9.

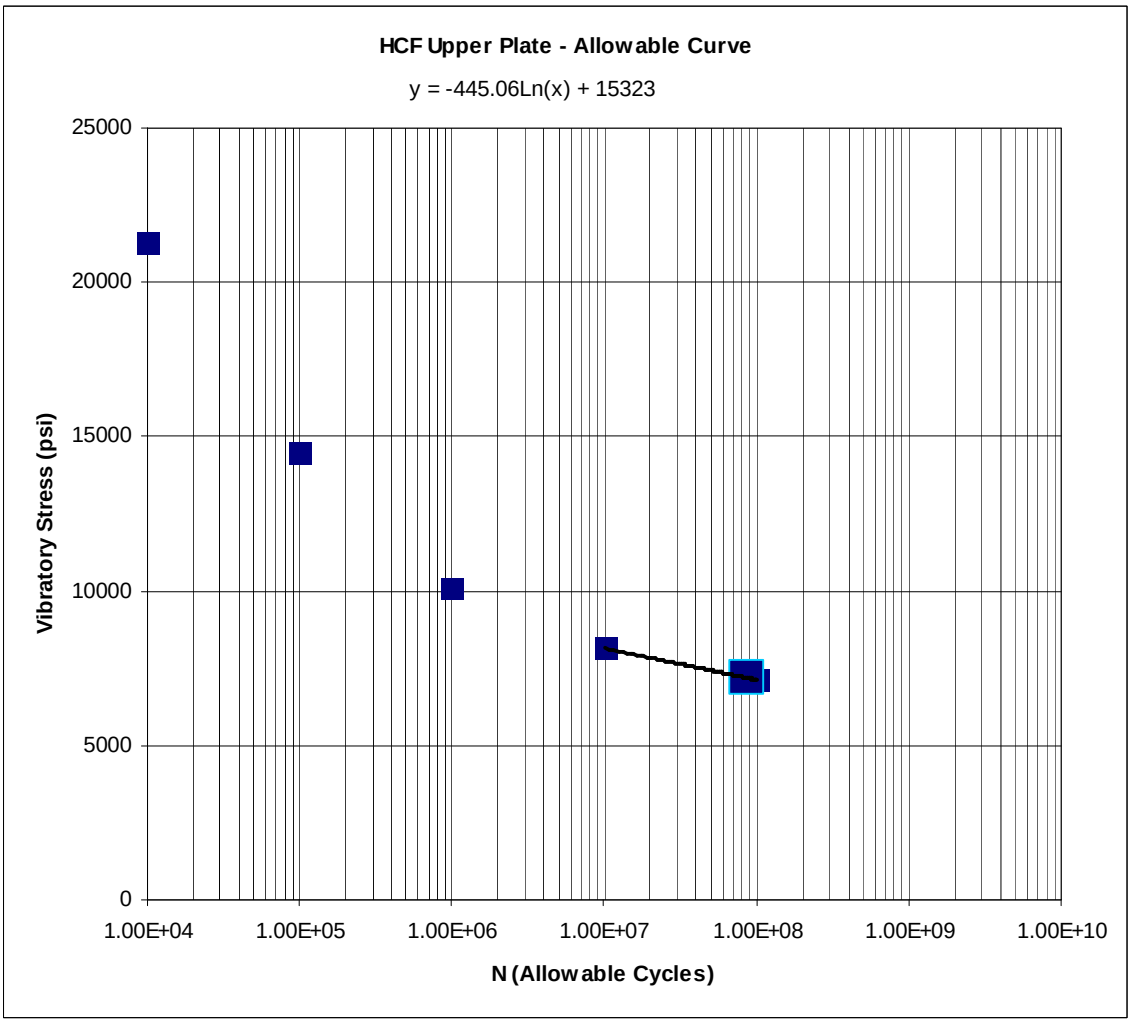

Figure 4.9 HCF Allowable Curve for Upper Hub Plate

Solving for *x* in the equation, the high cycle allowable number of cycles is 86,158,028. Now that an allowable number of cycles have been determined, the next step is to calculate the number of applied cycles for this condition in order to obtain the Miner's damage for this location. The high cycle load case is based upon the load occurrence of

1 per revolution. The rotational speed of the rotor is 413 rpm. The hub plates currently have a CRT of 2500 hours. The calculated number of applied cycles based upon the current CRT is given by the following equation:

$$\mathbf{2500\ hr * 413rpm * 60\ min/hr} \tag{4.4}$$

The applied number of cycles from the equation is 61,950,000. Therefore, the Miner's damage from high cycle loading for the upper hub plate is the number of applied cycles divided by the number of allowable cycles:

$$\mathbf{61{,}950{,}000 / 86{,}158{,}028 = 0.719} \tag{4.5}$$

The same process is required to establish the S/N curve for the upper hub plate from the low cycle fatigue (GAG) case. The steady stress value from the finite element model for the upper hub plate GAG condition is 20,943 psi and the oscillatory stress value is 12,362 psi. Taking the steady stress value, the corresponding oscillatory stress values are obtained from Figure 4.8 at each number of cycles shown on the graph. Shown in Table 4.4 is the allowable S/N calculation for the upper hub plate for the low cycle fatigue case.

Table 4.4 Allowable S/N Calculation for Upper Hub Plate LCF

N(cycles)	Stress (Osc)	K_f	K_{SF}	K_t	F_R	F_{SE}	$S_o(a)$
10000	43100	1	1	1	0.61	0.8	21032.8
100000	29000	1	1	1	0.61	0.8	14152
1000000	20200	1	1	1	0.61	0.8	9857.6
10000000	16400	1	1	1	0.61	0.8	8003.2
100000000	14000	1	1	1	0.61	0.8	6832

The oscillatory stress of 12,362 psi is between the fatigue allowable values of 14,152 and 9857.6 psi. This indicates that for the low cycle fatigue case for the upper hub plate, the allowable number of cycles is between 10^5 and 10^6 cycles. Plotting the allowable oscillatory stress values versus the number of cycles, a corresponding S/N curve will give a graphical representation in which Miner's damage can be calculated for this particular location and load case. Figure 4.10 is the S/N allowable curve for the upper hub plate subject to low cycle fatigue loading. The oscillatory stress value of 12,362 psi is indicated on the graph by a larger data point. This data point is calculated by generating a best fit curve between the data points for 10^5 and 10^6 cycles. This best fit curve gives an equation in which the allowable number of cycles can be calculated through a logarithmic linear interpolation. This equation is shown on the graph in Figure 4.10.

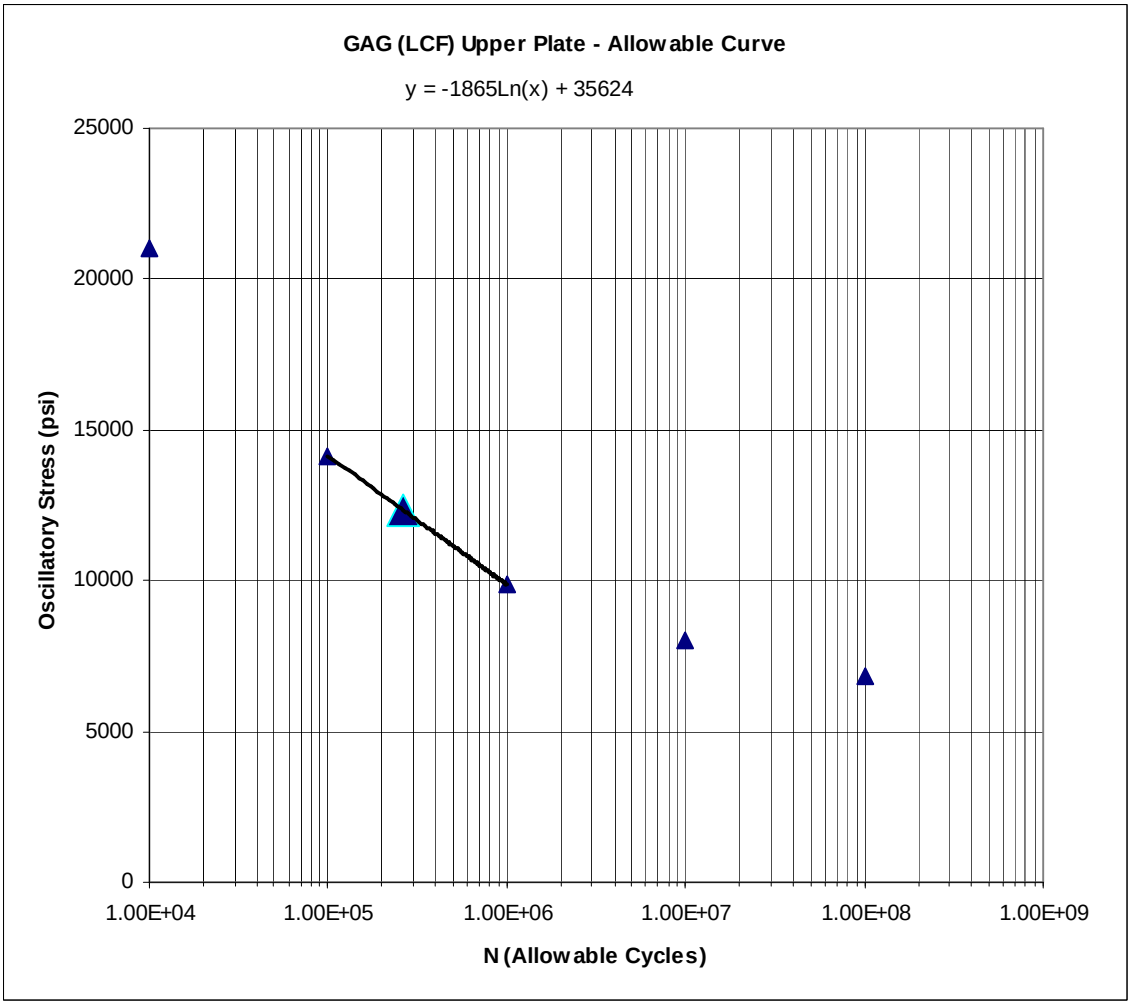

Figure 4.10 LCF Allowable Curve for Upper Hub Plate

Solving for *x* in the equation, the low cycle allowable number of cycles is 261,169. Now that an allowable number of cycles have been determined, the next step is to calculate the number of applied cycles for this condition in order to obtain the Miner's damage for this location. The low cycle load case is based upon the number of occurrences in the flight regime. Load case 2, which is used in the finite element model to represent the

low cycle fatigue condition, has a frequency of occurrence of 5 cycles per 1 flight hours. Again, we will use the current CRT of 2500 hours to calculate the number of applied cycles which is based on the following equation:

$$\mathbf{2500\ hr * 5\ cycles/hr = 12{,}500\ cycles} \tag{4.6}$$

Therefore, the Miner's damage from low cycle loading for the upper hub plate is the number of applied cycles divided by the number of allowable cycles:

$$\mathbf{12{,}500 / 261{,}169 = 0.048} \tag{4.7}$$

The total Miner's damage for the upper hub plate at this particular location is the sum of the damage form the high cycle and low cycle fatigue conditions.

$$\mathbf{0.719 + 0.048 = 0.767} \tag{4.8}$$

4.5 Miner's Damage Calculations for Lower Hub Plate

The same procedure is followed for the lower hub plate to establish the fatigue allowable stress values as was used for the upper hub plate. The S/N curve for the lower hub plate from the high cycle fatigue (HCF) case will be established first. The steady stress value from the finite element model for this condition is 19,170 psi and the oscillatory stress value is 7311 psi. Taking the steady stress value, the corresponding

oscillatory stress values are obtained from Figure 4.8 at each number of cycles shown on the graph. Shown in Table 4.5 is the allowable S/N calculation for the lower hub plate for the high cycle fatigue case.

Table 4.5 Allowable S/N Calculation for Lower Hub Plate HCF

N(cycles)	Stress (Osc)	K_f	K_{SF}	K_t	F_R	F_{SE}	$S_o(a)$
10000	44400	1	1	1	0.61	0.8	21667.2
100000	30200	1	1	1	0.61	0.8	14737.6
1000000	21100	1	1	1	0.61	0.8	10296.8
10000000	17000	1	1	1	0.61	0.8	8296
100000000	14900	1	1	1	0.61	0.8	7271.2

The oscillatory stress of 7311 psi is between the fatigue allowable values of 8296 and 7271.2 psi. This indicates that for the high cycle fatigue case for the lower hub plate, the allowable number of cycles is between 10^7 and 10^8 cycles. Plotting the allowable oscillatory stress values versus the number of cycles, a corresponding S/N curve will give a graphical representation in which Miner's damage can be calculated for this particular location and load case. Figure 4.11 is the S/N allowable curve for the lower hub plate subject to high cycle fatigue loading. The oscillatory stress value of 7311 psi is indicated on the graph by a larger data point. This data point is calculated by generating a best fit curve between the data points for 10^7 and 10^8 cycles. This best fit curve gives an equation in which the allowable number of cycles can be calculated through a logarithmic linear interpolation. This equation is shown on the graph in Figure 4.11.

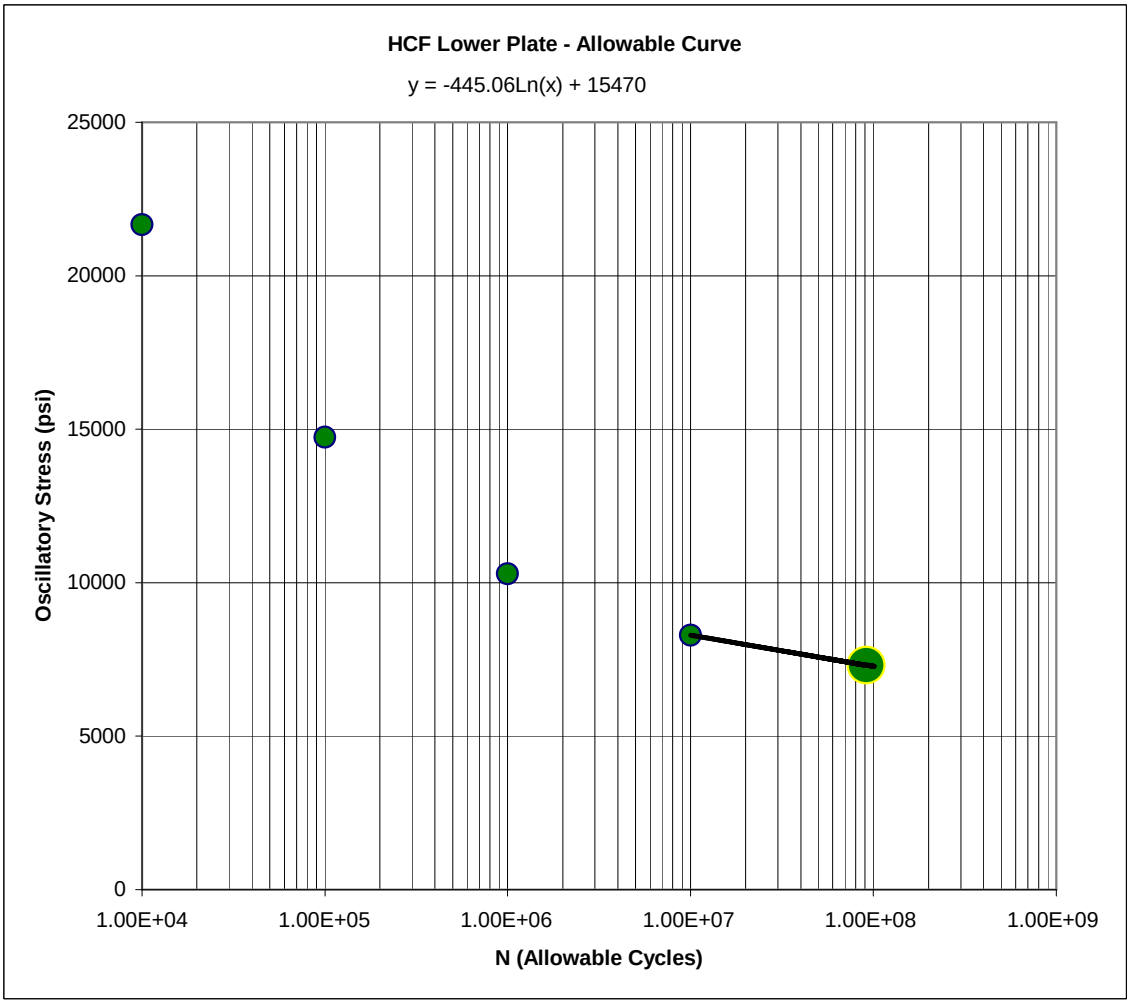

Figure 4.11 HCF Allowable Curve for Lower Hub Plate

Solving for *x* in the equation, the high cycle allowable number of cycles is 91,546,691. Now that an allowable number of cycles has been determined, the next step is to calculate the number of applied cycles for this condition in order to obtain the Miner's damage for this location. The high cycle load case is based upon the load occurrence of 1 per revolution. The rotational speed of the rotor is 413 rpm. The hub plates currently

have a CRT of 2500 hours. The calculated number of applied cycles based upon the current CRT is given by the following equation:

$$\mathbf{2500\ hr * 413rpm * 60\ min/hr} \tag{4.9}$$

The applied number of cycles from the equation is 61,950,000. Therefore, the Miner's damage from high cycle loading for the lower hub plate is the number of applied cycles divided by the number of allowable cycles:

$$\mathbf{61{,}950{,}000 / 91{,}546{,}691 = 0.677} \tag{4.10}$$

The same process is repeated to establish the S/N curve for the lower hub plate from the low cycle fatigue (GAG) case. The steady stress value from the finite element model for the lower hub plate GAG condition is 18,730 psi and the oscillatory stress value is 11,865 psi. Taking the steady stress value, the corresponding oscillatory stress values are obtained from Figure 4.8 at each number of cycles shown on the graph. Shown in Table 4.6 is the allowable S/N calculation for the lower hub plate for the low cycle fatigue case.

Table 4.6 Allowable S/N Calculation for Lower Hub Plate LCF

N(cycles)	Stress (Osc)	K_f	K_{SF}	K_t	F_R	F_{SE}	$S_o(a)$
10000	44600	1	1	1	0.61	0.8	21764.8
100000	30300	1	1	1	0.61	0.8	14786.4
1000000	21200	1	1	1	0.61	0.8	10345.6
10000000	17100	1	1	1	0.61	0.8	8344.8
100000000	15000	1	1	1	0.61	0.8	7320

The oscillatory stress of 11,865 psi is between the fatigue allowable values of 14,786.4 and 10,345.6 psi. This indicates that for the low cycle fatigue case for the lower hub plate, the allowable number of cycles is between 10^5 and 10^6 cycles. Plotting the allowable oscillatory stress values versus the number of cycles, a corresponding S/N curve will give a graphical representation in which Miner's damage can be calculated for this particular location and load case. Figure 4.12 is the S/N allowable curve for the lower hub plate subject to low cycle fatigue loading. The oscillatory stress value of 11,865 psi is indicated on the graph by a larger data point. This data point is calculated by generating a best fit curve between the data points for 10^5 and 10^6 cycles. This best fit curve gives an equation in which the allowable number of cycles can be calculated through a logarithmic linear interpolation. This equation is shown on the graph in Figure 4.12.

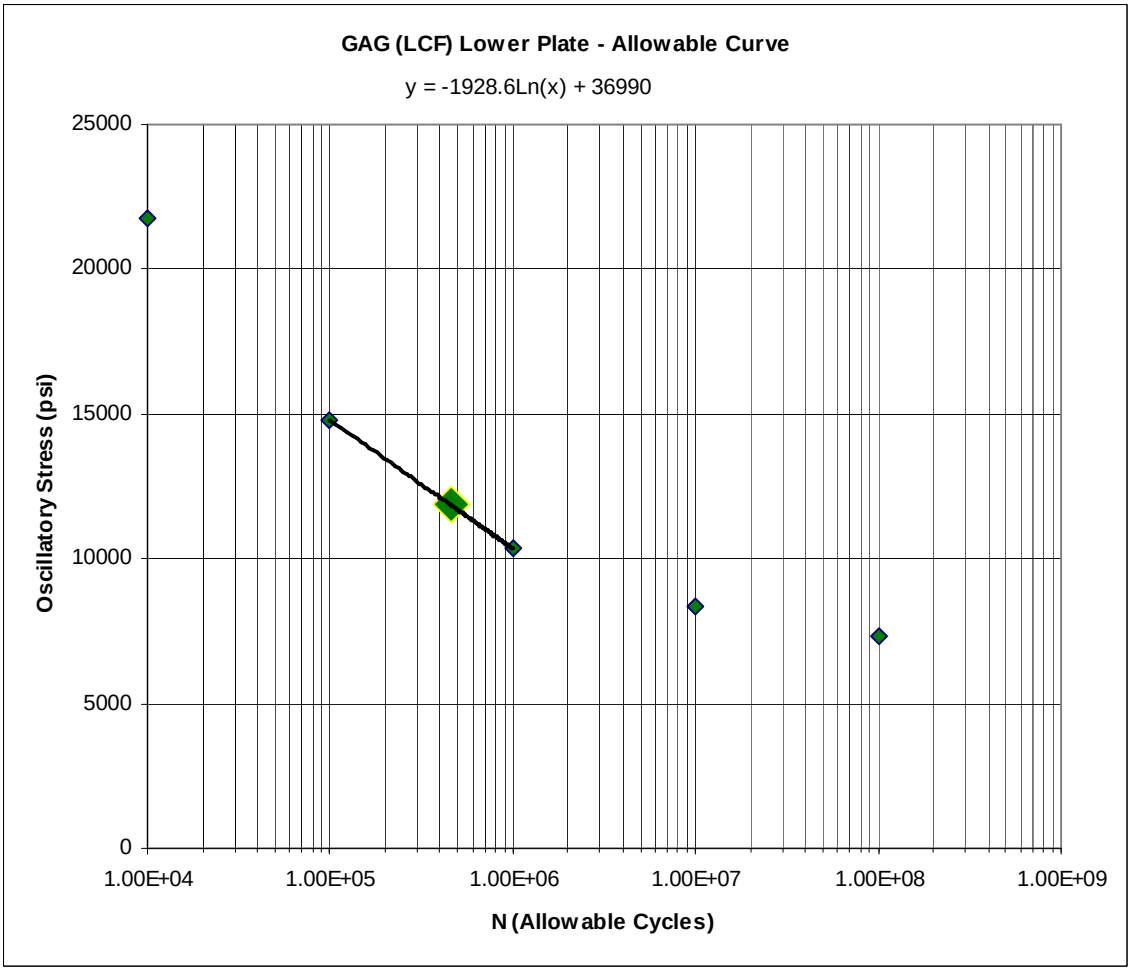

Figure 4.12 LCF Allowable Curve for Lower Hub Plate

Solving for *x* in the equation, the low cycle allowable number of cycles is 454,787. Now that an allowable number of cycles have been determined, the next step is to calculate the number of applied cycles for this condition in order to obtain the Miner's damage for this location. The low cycle load case is based upon the number of occurrences in the flight regime. Load case 2, which is used in the finite element model to represent the low cycle fatigue condition, has a frequency of occurrence of 5 cycles per 1 flight

hours. Again, we will use the current CRT of 2500 hours to calculate the number of applied cycles which is based on the following equation:

$$\mathbf{2500\ hr * 5\ cycles/hr = 12{,}500\ cycles} \tag{4.11}$$

Therefore, the Miner's damage from low cycle loading for the lower hub plate is the number of applied cycles divided by the number of allowable cycles:

$$\mathbf{12{,}500 / 454{,}787 = 0.027} \tag{4.12}$$

The total Miner's damage for the lower hub plate at this particular location is the sum of the damage form the high cycle and low cycle fatigue conditions.

$$\mathbf{0.677 + 0.027 = 0.704} \tag{4.13}$$

The total Miner's cumulative damage for the upper and lower hub plates has been calculated to be less than 1.0. This indicates that under the loading conditions evaluated in this project, the component will not experience fatigue failure if the recommended CRT is adhered to. It also indicates the component can have an increase in the CRT because the total Miner's damage is less than 1.0. The approximate safe life of the upper and lower hub plates is determined by the current designated life of 2500

hrs divided by the Miner's damage value of each component. This value is referred to as the crack initiation time (CIT) of the component.

Table 4.7 Miner's Damage Summary

Location	n/N (HCF)	n/N (LCF)	Total Miner's Damage	CIT Hours
Upper Hub Plate	0.719	0.048	0.767	3259
Lower Hub Plate	0.677	0.027	0.704	3551

The damage summary for the upper and lower hub plates as calculated by means of Miner's theory is presented in Table 4.7. The lower hub plate has a slightly higher CIT than the upper hub plate. This could be explained by the fact that the lower hub plate is bolted to the lower cone seat thereby increasing the overall stiffness in that region which would increase the amount of time necessary for a crack to occur. In any event, a conservative approach would be utilized, and the CRT of the upper and lower hub plates would be based on the lesser of the two values in order to facilitate replacement and maintainability issues.

CHAPTER 5

CONCLUSIONS AND RECOMMENDATIONS

5.1 Conclusions

The utility of an analytical evaluation on aircraft components in lieu of a full scale fatigue test has been investigated. The calculated results shown in Table 4.7, using measured flight loads as inputs, indicate that the fatigue life of the components analyzed can be increased from current published values. The results must be interpreted in light of the following assumptions. The first is that in the Miner's damage analysis for the high cycle fatigue case, it was assumed that the same maneuver was performed for the entire 2500 hours. This is a very conservative assumption since in reality this would never happen. The percentage of time in which load case 1 was actually performed is less than 2500 hours. Using this assumption, the Miner's damage from high cycle fatigue is also conservative. Therefore, the life expectances of the components in reality are higher than the calculated values shown in Table 4.7. In order to obtain a precise value from Miner's damage, numerous finite element iterations would need to be performed. There are literally hundreds of flight maneuvers included in the total flight spectrum. Performing a finite element analysis on a large number of high cycle load cases would not be a practical use of time nor would add much value to the outcome of the analysis.

The second assumption was made in the S/N curve calculations for the upper and lower hub plates. In the derivation of the S/N for the high cycle fatigue case only, the steady stress value that was used on the constant life fatigue diagram for aluminum was assumed to be the same for the entire high cycle fatigue load case. This also is conservative since the steady stress will vary with the various flight maneuvers. The effect of a lower steady stress will increase the allowable oscillatory stress, which also increases the allowable number of cycles for the component, thereby decreasing Miner's damage.

The results indicate that the finite element analysis performed was a useful method in determining the life expectancy of the upper and lower hub plates. The steady and oscillatory stress values obtained in the analysis were represented on the Soderberg diagram which indicated that the life expectancy of the components is determined by fatigue factors. The accuracy of the applied loads was verified through the comparison of measured flight data for mast torque and the extracted moment reaction of a fixed boundary location of the mast in the finite element model.

5.2 Recommendations

Upon the completion of the finite element analysis, there are two approaches which could be pursued to extend the work described here. The first approach would be to obtain more flight data and perform additional finite element analysis on a large number of high cycle fatigue conditions encountered in the total flight spectrum. This could lead to a less conservative Miner's damage estimate.

The second approach would be to perform a full scale laboratory fatigue test of the main rotor system in which the upper and lower hub plates are the focal point of damage determination. At this point, this is probably the most practical approach since there is now analytical data to suggest the suitability of a full scale test. Which course is taken for further study would be determined through a joint effort between the FAA and senior management.

REFERENCES

[1] Pegoretti, A. 2001. “Finite Element analysis of a glass fiber reinforced composite endodontic post”, Biomaterials, Volume 23, Issue 13, pg 2667-2682

[2] Silva, M., T. Keaveny, W. Hayes 2005. “Computed tomography-based finite element analysis predicts failure loads and fracture patterns for vertebral sections”, Journal of Orthopaedic Research, Vol 16 Issue 3, pg 300-308.

[3] Savaidis, G. and M. Vormwald 2000. “Hot spot stress evaluation of fatigue in welded structural connections supported by finite element analysis”, International Journal of Fatigue, Volume 22, Issue 2, pg 85-91.

[4] Chan, T., L. Guo and Z. X. Li 2003. “Finite element modeling for fatigue stress analysis of large suspension bridges”, Journal of Sound and Vibration, Volume 261, Issue 3, pg 443-464.

[5] Schaff, J., A. Dobyns 1998. “Fatigue analysis of helicopter tail rotor spar” AIAA Structural Dynamics and Materials Conference and Exhibit, Long Beach CA, 20-23 Apr 1998.

[6] Colombo, D., M. Giglio 2007 “Determination of the fatigue life of a helicopter tail rotor transmission subjected to ballistic damage”, Engineering Fracture Mechanics, Volume 74, Issue 4, pg 481-499.

[7] Montgomery, J., “Helicopter Flight Theory for Pilots and Mechanics”, Sikorsky Aircraft, pg 37-38, June 1974.

[8] www.ansys.com/products/default, obtained Nov 11, 2008.

[9] Society of Automotive Engineers 2003, “Impulse Testing of Aerospace Hydraulic Actuators, Valves, Pressure Containers, and Similar Fluid System Components” ARP 1383 Rev B, pg 1-2, Feb 2003.

[10] Altman, B. 2003, “Guidelines for Fatigue Substantiation Based on Laboratory and Flight Test Data”, Sikorsky Aircraft, Rev B, pg 234-250, Aug 2003.

[11] “Structural Design Manual”, Bell Helicopter Textron, Volume 1, Section 7, pg 17-32, July 1989.

[12] Hunter, D. 2007, “Analytical Fatigue Evaluation Methodology Report for Dynamic Systems Structure”, Sikorsky Aircraft, Rev A, pg 23-44, Sep 2007.

[13] “Structural Design Manual”, Bell Helicopter Textron, Volume 2, Section 3, pg 77-94, July 1989.

[14] Aerospace Material Specification, “Shot Peening of Metal Parts” AMS-S-13165 Rev A, pg 3, Dec 2007.

BIOGRAPHICAL INFORMATION

Douglas Wittig received his Bachelor of Science in Mechanical Engineering from the State University of New York at Buffalo. After his undergraduate studies, he went on to work in the field of heat transfer for seven years as a design and applications engineer. Mr. Wittig was involved in the mechanical and thermal design of commercial and industrial heat exchangers which were used in the pipeline after-cooler, oil cooler, steam condensers, and co-generation industry. He then went on to work in the field of power generation for four years as a project manager and supervisor for Caterpillar Inc. He primarily engaged in design and supply of power generators for land and offshore oil drilling companies such as Shell, BP, Exxon, Marathon, and Kerr McGee.

Douglas entered the aerospace field in 2004 at Bell Helicopter. Mr. Wittig worked as a stress analyst for the propulsion group and also the rotors group in which he worked on multiple commercial and military programs. He is currently working at Sikorsky Aircraft as a stress analyst in the rotors group focusing his time on a prototype design for the military and also a new product development commercial aircraft. He started his graduate studies in 2004 at the University of Texas at Arlington and earned Master of Science in Mechanical Engineering degree in December 2008.